

1 **Effects of elevated CO<sub>2</sub> and temperature on phytoplankton community**  
2 **biomass, species composition and photosynthesis during an autumn**  
3 **bloom in the Western English Channel**

4 Matthew Keys<sup>1,2</sup>, Gavin Tilstone<sup>1\*</sup>, Helen S. Findlay<sup>1</sup>, Claire E. Widdicombe<sup>1</sup> and Tracy Lawson<sup>2</sup>.

5 <sup>1</sup> Plymouth Marine Laboratory, Prospect Place, The Hoe, Plymouth, PL1 3DH, UK.

6 <sup>2</sup> University of Essex, Wivenhoe Park, Colchester, CO4 3SQ, UK.

7 *Correspondence to:* G. Tilstone (ghti@pml.ac.uk)

8

9 **Abstract**

10 The combined effects of elevated pCO<sub>2</sub> and temperature were investigated during an autumn  
11 phytoplankton bloom in the Western English Channel (WEC). A full factorial 36-day microcosm  
12 experiment was conducted under year 2100 predicted temperature (+ 4.5 °C) and pCO<sub>2</sub> levels  
13 (800 µatm). The starting phytoplankton community biomass was 110.2 (± 5.7 sd) mg carbon (C)  
14 m<sup>-3</sup> and was dominated by dinoflagellates (~50 %) with smaller contributions from  
15 nanophytoplankton (~13 %), cryptophytes (~11 %) and diatoms (~9 %). Over the experimental  
16 period total phytoplankton biomass was significantly increased by elevated pCO<sub>2</sub> (20-fold) and  
17 at the end of the experiment, biomass also increased under elevated temperature (15-fold). By  
18 contrast, the combined influence of elevated pCO<sub>2</sub> and temperature had little effect on biomass  
19 relative to the control. Throughout the experiment in all treatments, the phytoplankton  
20 community structure shifted from dinoflagellates to nanophytoplankton. At the end of the  
21 experiment, under elevated pCO<sub>2</sub> nanophytoplankton contributed 90% of community biomass  
22 and was dominated by *Phaeocystis* spp.. Under elevated temperature, nanophytoplankton  
23 comprised 85% of the community biomass and was dominated by smaller nano-flagellates. In  
24 the control, larger nano-flagellates dominated whilst the smallest nanophytoplankton  
25 contribution was observed under combined elevated pCO<sub>2</sub> and temperature (~40 %). Under  
26 elevated pCO<sub>2</sub>, temperature and in the control, there was a significant decrease in dinoflagellate  
27 biomass. Under the combined effects of elevated pCO<sub>2</sub> and temperature, dinoflagellate biomass  
28 almost doubled from the starting value and there was a 30-fold increase in the harmful algal  
29 bloom (HAB) species, *Prorocentrum cordatum*. At the end of experiment, Chlorophyll a (Chl a)  
30 normalised maximum photosynthetic rates (P<sup>B<sub>m</sub></sup>) increased > 6-fold under elevated pCO<sub>2</sub> and >  
31 3-fold under elevated temperature while no effect on P<sup>B<sub>m</sub></sup> was observed when pCO<sub>2</sub> and  
32 temperature were elevated simultaneously. The results suggest that future increases in

33 temperature and pCO<sub>2</sub> simultaneously do not appear to influence coastal phytoplankton  
34 productivity during autumn in the WEC which would have a negative feedback on atmospheric  
35 CO<sub>2</sub>.

## 36 **1. Introduction**

37 Oceanic concentration of CO<sub>2</sub> has increased by ~42% over pre-industrial levels, with a  
38 continuing annual increase of ~0.4%. Current CO<sub>2</sub> level has reached ~400 μatm and has been  
39 predicted to rise to >700 μatm by the end of this century (IPCC, 2013), with estimates exceeding  
40 1000 μatm (Matear and Lenton, 2018; Raupach et al., 2007; Raven et al., 2005). With increasing  
41 atmospheric CO<sub>2</sub>, the oceans continue to absorb CO<sub>2</sub> from the atmosphere, which results in a  
42 shift in oceanic carbonate chemistry resulting in a decrease in seawater pH or 'Ocean  
43 Acidification' (OA). The projected increase in atmospheric CO<sub>2</sub> and corresponding increase in  
44 ocean uptake, is predicted to result in a decrease in global mean surface seawater pH of 0.3  
45 units below the present value of 8.1 to 7.8 (Wolf-gladrow et al., 1999). Under this scenario, the  
46 shift in dissolved inorganic carbon (DIC) equilibria has wide ranging implications for  
47 phytoplankton photosynthetic carbon fixation rates and growth (Riebesell, 2004).

48 Concurrent with OA, elevated atmospheric CO<sub>2</sub> and other climate active gases have warmed the  
49 planet by ~0.6 °C over the past 100 years (IPCC, 2007). Atmospheric temperature has been  
50 predicted to rise by a further 1.8 to 4 °C by the end of this century (Alley et al., 2007).

51 Phytoplankton metabolic activity may be accelerated by increased temperature (Eppley, 1972),  
52 which can vary depending on the phytoplankton species and their physiological  
53 requirements (Beardall et al., 2009; Boyd et al., 2013). Long-term data sets already suggest that  
54 ongoing changes in coastal phytoplankton communities are likely due to climate shifts and other  
55 anthropogenic influences (Edwards et al., 2006; Smetacek and Cloern, 2008; Widdicombe et al.,  
56 2010). The response to OA and temperature can potentially alter the community composition,  
57 community biomass and photo-physiology. Understanding how these two factors may interact,  
58 synergistically or antagonistically, is critical to our understanding and for predicting future  
59 primary productivity (Boyd and Doney, 2002; Dunne, 2014).

60 Laboratory studies of phytoplankton species in culture and studies on natural populations in  
61 the field have shown that most species exhibit sensitivity, in terms of growth and  
62 photosynthetic rates, to elevated pCO<sub>2</sub> and temperature individually. To date, only a few studies  
63 have investigated the interactive effects of these two parameters on natural populations (e.g.  
64 Coello-Camba et al., 2014; Feng et al., 2009; Gao et al., 2017; Hare et al., 2007). Most laboratory  
65 studies demonstrate variable results with species-specific responses. In the diatom  
66 *Thalassiosira weissflogii* for example, pCO<sub>2</sub> elevated to 1000 μatm and + 5 °C temperature

67 synergistically enhanced growth, while the same conditions resulted in a reduction in growth  
68 for the diatom *Dactyliosolen fragilissimus* (Taucher et al., 2015). Although there have been fewer  
69 studies on dinoflagellates, variable responses have also been reported (Errera et al., 2014; Fu et  
70 al., 2008). In natural populations, elevated pCO<sub>2</sub> has stimulated the growth of pico- and  
71 nanophytoplankton (Boras et al., 2016; Engel et al., 2008) while increased temperature has  
72 reduced their biomass (Moustaka-Gouni et al., 2016; Peter and Sommer, 2012). In a recent field  
73 study on natural phytoplankton communities, elevated temperature (+ 3°C above ambient)  
74 enhanced community biomass but the combined influence of elevated temperature and pCO<sub>2</sub>  
75 reduced the biomass (Gao et al., 2017).

76 Phytoplankton species composition, abundance and biomass has been measured since 1992 at  
77 the time-series station L4 in the western English Channel (WEC), to evaluate how global  
78 changes could drive future shifts in phytoplankton community structure and carbon  
79 biogeochemistry. At this station, sea surface temperature and pCO<sub>2</sub> reach maximum values  
80 during late summer and start to decline in autumn. During October, mean seawater  
81 temperatures at 10 m decrease from 15.39 °C (± 0.49 sd) to 14.37 °C (± 0.62 sd). Following a  
82 period of CO<sub>2</sub> oversaturation in late summer, pCO<sub>2</sub> returns to near-equilibrium at station L4 in  
83 October when mean pCO<sub>2</sub> values decrease from 455.32 µatm (± 63.92 sd) to 404.06 µatm (±  
84 38.55 sd) (Kitidis et al., 2012).

85 From a biological perspective, the autumn period at station L4 is characterised by the decline of  
86 the late summer diatom and dinoflagellate blooms (Widdicombe et al., 2010) when their  
87 biomass approaches values close to the time series minima (diatom biomass range: 6.01 (± 6.88  
88 sd) – 2.85 (± 3.28 sd) mg C m<sup>-3</sup>; dinoflagellate biomass range: 1.75 (± 3.28 sd) – 0.66 (± 1.08 sd)  
89 mg C m<sup>-3</sup>). Typically, over this period nanophytoplankton becomes numerically dominant and  
90 biomass ranges from 20.94 (± 33.25 sd) – 9.38 (± 3.31 sd) mg C m<sup>-3</sup>, though there is  
91 considerable variability in this biomass.

92 Based on the existing literature, the working hypotheses of this study are that: (1) community  
93 biomass will increase differentially under individual treatments of elevated temperature and  
94 pCO<sub>2</sub>; (2) elevated pCO<sub>2</sub> will lead to taxonomic shifts due to differences in species-specific CO<sub>2</sub>  
95 concentrating mechanisms and/or RuBisCO specificity; (3) photosynthetic carbon fixation rates  
96 will increase differentially under individual treatments of elevated temperature and pCO<sub>2</sub>; (4)  
97 elevated temperature will lead to taxonomic shifts due to species-specific thermal optima; (5)  
98 temperature and pCO<sub>2</sub> elevated simultaneously will have synergistic effects.

99 The objective of the study was therefore to investigate the combined effects of elevated pCO<sub>2</sub>  
100 and temperature on phytoplankton community structure, biomass and photosynthetic carbon

101 fixation rates during the autumn transition from diatoms and dinoflagellates to  
102 nanophytoplankton at station L4 in the WEC.

## 103 **2. Materials and methods**

### 104 **2.1 Perturbation experiment, sampling and experimental set-up**

105 Experimental seawater containing a natural phytoplankton community was sampled at station  
106 L4 (50 ° 15' N, 4 ° 13' W) on 7<sup>th</sup> October 2015 from 10 m depth (40 L). The experimental  
107 seawater was gently pre-filtered through a 200 µm Nitex mesh to remove zooplankton grazers,  
108 into two 20 L acid-cleaned carboys. While grazers play an important role in regulating  
109 phytoplankton community structure (e.g. Strom, 2002), our experimental goals considered only  
110 the effects of elevated temperature and pCO<sub>2</sub>. In addition, 320 L of seawater was collected into  
111 sixteen 20 L acid-cleaned carboys from the same depth for use as experimental media.  
112 Immediately upon return to the laboratory the media seawater was filtered through an in-line  
113 0.2 and 0.1 µm filter (Acropak™, Pall Life Sciences) then stored in the dark at 14 °C until use. The  
114 experimental seawater was gently and thoroughly mixed and transferred in equal parts from  
115 each carboy (to ensure homogeneity) to sixteen 2.5 L borosilicate incubation bottles (4 sets of 4  
116 replicates). The remaining experimental seawater was sampled for initial (T0) concentrations of  
117 nutrients, Chl *a*, total alkalinity, dissolved inorganic carbon, particulate organic carbon (POC)  
118 and nitrogen (PON) and was also used to characterise the starting experimental phytoplankton  
119 community. The incubation bottles were placed in an outdoor simulated in-situ incubation  
120 culture system and each set of replicates was linked to one of four 22 L reservoirs filled with the  
121 filtered seawater media. Neutral density spectrally corrected blue filters (Lee Filter no. 061)  
122 were placed between polycarbonate sheets and mounted to the top, sides and ends of the  
123 incubation system to provide ~50 % irradiance, approximating PAR measured at 10 m depth at  
124 station L4 on the day of sampling prior to starting experimental incubations (see **Fig. S1**,  
125 supplementary material for time course of PAR levels during the experiment). The media was  
126 aerated with CO<sub>2</sub> free air and 5 % CO<sub>2</sub> in air precisely mixed using a mass flow controller  
127 (Bronkhorst UK Limited) and used for the microcosm dilutions as per the following  
128 experimental design: (1) control (390 µatm pCO<sub>2</sub>, 14.5 °C matching station L4 in-situ values),  
129 (2) high temperature (390 µatm pCO<sub>2</sub>, 18.5 °C), (3) high pCO<sub>2</sub> (800 µatm pCO<sub>2</sub>, 14.5 °C) and (4)  
130 combination (800 µatm pCO<sub>2</sub>, 18.5 °C).

131 Initial nutrient concentrations (0.24 µM nitrate + nitrite, 0.086 µM phosphate and 2.14 µM  
132 silicate on 7<sup>th</sup> October 2015) were amended to 8 µM nitrate+nitrite and 0.5 µM phosphate.  
133 Pulses of nutrient inputs frequently occur at station L4 from August to December following  
134 heavy rainfall events and subsequent riverine inputs to the system (e.g. Barnes et al., 2015). Our

135 nutrient amendments simulated these in situ conditions and were held constant to maintain  
136 phytoplankton growth. Previous pilot studies highlighted that if these concentrations were not  
137 maintained, the phytoplankton population crashes (Keys, 2017). As the phytoplankton  
138 community was sampled over the transitional phase from diatoms and dinoflagellates to  
139 nanophytoplankton, the in situ silicate concentration was maintained to reproduce the silicate  
140 concentrations typical of this time of year (Smyth et al., 2010). The experiment formed part of a  
141 PhD study with limitations on resources and training for nutrients analysis. Nutrient  
142 concentrations were measured at time point T0 only.

143 Media transfer and sample acquisition was driven by peristaltic pumps. Following 48 hrs  
144 acclimation in batch culture, semi-continuous daily dilution rates were maintained at between  
145 10-13 % of the incubation bottle volume throughout the experiment. CO<sub>2</sub> enriched seawater  
146 was added to the high CO<sub>2</sub> treatment replicates every 24 hrs, acclimating the natural  
147 phytoplankton population to increments of elevated pCO<sub>2</sub> from ambient to ~800 µatm over 8  
148 days followed by maintenance at ~800 µatm as per the method described by Schulz *et al*,  
149 (2009). Adding CO<sub>2</sub> enriched seawater is the preferred protocol, since some phytoplankton  
150 species are inhibited by the mechanical effects of direct bubbling (Riebesell et al., 2010; Shi et  
151 al., 2009) which causes a reduction in growth rates and the formation of aggregates (Love et al.,  
152 2016). pH was monitored daily to adjust the pCO<sub>2</sub> of the experimental media (+/-) prior to  
153 dilutions to maintain target pCO<sub>2</sub> levels in the incubation bottles. The seasonality in pH and total  
154 alkalinity (TA) are fairly stable at station L4 with high pH and low dissolved inorganic carbon  
155 (DIC) during early summer, and low pH, high DIC throughout autumn and winter (Kitidis et al.,  
156 2012). By maintaining the carbonate chemistry over the duration of the experiment, we aimed  
157 to simulate natural events at the study site.

158 To provide sufficient time for changes in the phytoplankton community to occur and to achieve  
159 an ecologically relevant data set, the incubation period was extended well beyond short-term  
160 acclimation. Previous pilot studies using the same experimental protocols highlighted that after  
161 ~20 days of incubation, significant changes in community structure and biomass were observed  
162 (Keys, 2017). These results were used to inform a more relevant incubation period of 30+ days.

## 163 **2.2 Analytical methods, experimental seawater**

### 164 **2.2.1 Chlorophyll *a***

165 Chl *a* was measured in each incubation bottle. 100 mL triplicate samples from each replicate  
166 were filtered onto 25 mm GF/F filters (nominal pore size 0.7 µm), extracted in 90 % acetone  
167 overnight at -20 °C and Chl *a* concentration was measured on a Turner Trilogy™ fluorometer  
168 using the non-acidified method of Welschmeyer (1994). The fluorometer was calibrated against

169 a stock Chl *a* standard (*Anacystis nidulans*, Sigma Aldrich, UK), the concentration of which was  
170 determined with a Perkin Elmer™ spectrophotometer at wavelengths 663.89 and 750.11 nm.  
171 Samples for Chl *a* analysis were taken every 2-3 days.

### 172 **2.2.2 Carbonate system**

173 70 mL samples for total alkalinity (TA) and dissolved inorganic carbon (DIC) analysis were  
174 collected from each experimental replicate, stored in amber borosilicate bottles with no head  
175 space and fixed with 40 µL of super-saturated Hg<sub>2</sub>Cl<sub>2</sub> solution for later determination (Apollo  
176 SciTech™ Alkalinity Titrator AS-ALK2; Apollo SciTech™ AS-C3 DIC analyser, with analytical  
177 precision of 3 µmol kg<sup>-1</sup>). Duplicate measurements were made for TA and triplicate  
178 measurements for DIC. Carbonate system parameter values for media and treatment samples  
179 were calculated from TA and DIC measurements using the programme CO<sub>2</sub>sys (Pierrot et al.,  
180 2006) with dissociation constants of carbonic acid of Mehrbach *et al.*, (1973) refitted by Dickson  
181 and Millero (Dickson and Millero, 1987). Samples for TA and DIC were taken for analysis every  
182 2-3 days throughout the experiment.

### 183 **2.2.3 Phytoplankton community analysis**

184 Phytoplankton community analysis was performed by flow cytometry (Becton Dickinson Accuri  
185 ™ C6) for the 0.2 to 18 µm size fraction following Tarran *et al.*, (2006) and inverted light  
186 microscopy was used to enumerate cells > 18 µm (BS EN 15204,2006). For flow cytometry, 2  
187 mL samples fixed with glutaraldehyde to a final concentration of 2 % were flash frozen in liquid  
188 nitrogen and stored at -80 °C for subsequent analysis. Phytoplankton data acquisition was  
189 triggered on both chlorophyll fluorescence and forward light scatter (FSC) using prior  
190 knowledge of the position of *Synechococcus* sp. to set the lower limit of analysis. Density plots of  
191 FSC vs. CHL fluorescence, phycoerythrin fluorescence vs. CHL fluorescence and side scatter  
192 (SSC) vs. CHL fluorescence were used to discriminate *Synechococcus* sp., picoeukaryote  
193 phytoplankton (approx. 0.5–3 µm), coccolithophores, cryptophytes, *Phaeocystis* sp. single cells  
194 and nanophytoplankton (eukaryotes >3 µm, excluding the coccolithophores, cryptophytes and  
195 *Phaeocystis* sp. single cells). For inverted light microscopy, 140 mL samples were fixed with 2 %  
196 (final concentration) acid Lugol's iodine solution and analysed by inverted light microscopy  
197 (Olympus™ IMT-2) using the Utermöhl counting technique (Utermöhl, 1958; Widdicombe *et al.*,  
198 2010). Phytoplankton community samples were taken at T0, T10, T17, T24 and T36.

### 199 **2.2.4 Phytoplankton community biomass**

200 The smaller size fraction identified and enumerated through flow cytometry;  
201 picophytoplankton, nanophytoplankton, *Synechococcus*, coccolithophores and cryptophytes

202 were converted to carbon biomass ( $\text{mg C m}^{-3}$ ) using a spherical model to calculate mean cell  
203 volume:

$$204 \left(\frac{4}{3} * \pi * r^3\right) \quad \text{Equation 1.}$$

205 and a conversion factor of  $0.22 \text{ pg C } \mu\text{m}^{-3}$  (Booth, 1988). A conversion factor of  $0.285 \text{ pg C } \mu\text{m}^{-3}$   
206 was used for coccolithophores (Tarran et al., 2006) and cell a volume of  $113 \mu\text{m}^3$  and carbon  
207 cell<sup>-1</sup> value of  $18 \text{ pg}$  applied for *Phaeocystis* spp. (Widdicombe et al., 2010). *Phaeocystis* spp.  
208 were identified and enumerated by flow cytometry separately to the nanophytoplankton class  
209 due to high observed abundance in in the high pCO<sub>2</sub> treatment. Mean cell measurements of  
210 individual species/taxa were used to calculate cell bio-volume for the  $18 \mu\text{m} +$  size fraction  
211 according to Kovalala and Larrance (1966) and converted to biomass according to the equations  
212 of Menden-Deuer & Lessard, (2000).

### 213 **2.2.5 POC and PON**

214 Samples for particulate organic carbon (POC) and particulate organic nitrogen (PON) were  
215 taken at T0, T15 and T36.150 mL samples were taken from each replicate and filtered under  
216 gentle vacuum pressure onto pre-ashed 25mm glass fibre filters (GF/F, nominal pore size  $0.7$   
217  $\mu\text{m}$ ). Filters were stored in acid washed petri-slides at  $-20 \text{ }^\circ\text{C}$  until further processing. Sample  
218 analysis was conducted using a Thermoquest Elemental Analyser (Flash 1112). Acetanilide  
219 standards (Sigma Aldrich, UK) were used to calibrate measurements of carbon and nitrogen and  
220 also used during the analysis to account for possible drift in measured concentrations.

### 221 **2.2.6 Chl fluorescence-based photophysiology**

222 Photosystem II (PSII) variable chlorophyll fluorescence parameters were measured using a fast  
223 repetition rate fluorometer (FRRf) (FastOcean sensor in combination with an Act2Run  
224 laboratory system, Chelsea Technologies, West Molesey, UK). The excitation wavelengths of the  
225 FRRf's light emitting diodes (LEDs) were  $450, 530$  and  $624 \text{ nm}$ . The instrument was used in  
226 single turnover mode with a saturation phase comprising  $100$  flashlets on a  $2 \mu\text{s}$  pitch and a  
227 relaxation phase comprising  $40$  flashlets on a  $50 \mu\text{s}$  pitch. Measurements were conducted in a  
228 temperature-controlled chamber at  $15 \text{ }^\circ\text{C}$ . The minimum ( $F_0$ ) and maximum ( $F_m$ ) Chl  
229 fluorescence were estimated according to Kolber et al., (1998). Maximum quantum yields of PSII  
230 were calculated as:

$$231 F_v / F_m = (F_m - F_0) / F_m \quad \text{Equation 2.}$$

232 PSII electron flux was calculated on a volume basis ( $\text{JV}_{\text{PSII}}$ ;  $\text{mol e}^- \text{ m}^{-3} \text{ d}^{-1}$ ) using the absorption  
233 algorithm (Oxborough et al., 2012) following spectral correction by normalising the FRRf LED

234 emission to the white spectra using Fast<sup>PRO</sup> 8 software. This step required inputting the  
235 experimental phytoplankton community fluorescence excitation spectra values (FES). Since we  
236 did not measure the FES of our experimental samples, we used mean literature values for each  
237 phytoplankton group calculated proportionally (based on percentage contribution to total  
238 estimated biomass per phytoplankton group) as representative values for our experimental  
239 samples. The  $JV_{PSII}$  rates were converted to chlorophyll specific carbon fixation rates ( $\text{mg C (mg}$   
240  $\text{Chl } a)^{-1} \text{ m}^{-3} \text{ h}^{-1}$ ), calculated as:

$$241 \quad J_{V_{PSII}} \times \varphi_{E:C} \times MW_C / \text{Chl } a \quad \text{Equation 3}$$

242 where  $\varphi_{E:C}$  is the electron requirement for carbon uptake ( $\text{molecule CO}_2 \text{ (mol electrons)}^{-1}$ ),  $MW_C$   
243 is the molecular weight of carbon and  $\text{Chl } a$  is the  $\text{Chl } a$  measurement specific to each sample.  
244  $\text{Chl } a$  specific  $J_{V_{PSII}}$  based photosynthesis-irradiance curves were conducted in replicate batches  
245 between 10:00 – 16:00 to account for variability over the photo-period at between 8 - 14  
246 irradiance intensities. The maximum intensity applied was adjusted according to ambient  
247 natural irradiance on the day of sampling. Maximum photosynthetic rates of carbon fixation  
248 ( $P^B_m$ ), the light limited slope ( $\alpha^B$ ) and the light saturation point of photosynthesis ( $I_k$ ) were  
249 estimated by fitting the data to the model of Webb et al., (1974):

$$250 \quad P^B = (1 - e^{-\alpha \times I / P^B_m}) \quad \text{Equation 4}$$

251 Due to instrument failure during the experiment, samples for FRRf fluorescence-based light  
252 curves were taken at T36 only.

### 253 **2.3 Statistical analysis**

254 To test for effects of temperature,  $p\text{CO}_2$  and possible time dependence of the measured response  
255 variables ( $\text{Chl } a$ , total biomass, POC, PON, photosynthetic parameters and biomass of individual  
256 species), generalized linear mixed models with the factors  $p\text{CO}_2$ , temperature and time (and all  
257 interactions) were applied to the data between T0 and T36. Analyses were conducted using the  
258 lme4 package in R (R Core Team (2014). R Foundation for Statistical Computing, Vienna,  
259 Austria).

## 260 **3. Results**

261  $\text{Chl } a$  concentration in the WEC at station L4 from 30 September - 6<sup>th</sup> October 2015 (when sea  
262 water was collected for the experiment) varied between  $0.02\text{-}5 \text{ mg m}^{-3}$ , with a mean  
263 concentration of  $\sim 1.6 \text{ mg m}^{-3}$  (**Fig. 1 A**). Over the period leading up to phytoplankton  
264 community sampling, increasing nitrate and silicate concentrations coincided with a  $\text{Chl } a$  peak  
265 on 23<sup>rd</sup> September (**Fig. 1 B**). Routine net trawl ( $20 \mu\text{m}$ ) sample observations indicated a  
266 phytoplankton community dominated by the diatoms *Leptocylindrus danicus* and *L. minimus*



267 with a lower presence of the dinoflagellates *Prorocentrum cordatum*, *Heterocapsa* spp. and  
268 *Oxytoxum gracile*. Following decreasing nitrate concentrations, there was a *P. cordatum* bloom  
269 on 29<sup>th</sup> September, during the week before the experiment started (data not shown).

### 270 **3.1 Experimental carbonate system**

271 Equilibration to the target high pCO<sub>2</sub> values (800 µatm) within the high pCO<sub>2</sub> and combination  
272 treatments was achieved at T10 (**Fig. 2 A & B**). These treatments were slowly acclimated to  
273 increasing levels of pCO<sub>2</sub> over 7 days (from the initial dilution at T3) while the control and high  
274 temperature treatments were acclimated at the same ambient carbonate system values as those  
275 measured at station L4 on the day of sampling. Following equilibration, the mean pCO<sub>2</sub> values  
276 within the control and high temperature treatments were 394.9 (± 4.3 sd) and 393.2 (± 4.8 sd)  
277 µatm respectively, while in the high pCO<sub>2</sub> and combination treatments mean pCO<sub>2</sub> values were  
278 822.6 (± 9.4) and 836.5 (± 15.6 sd) µatm, respectively. Carbonate system values remained stable  
279 throughout the experiment (For full carbonate system measured and calculated parameters, see  
280 **Table S1** in supplementary material).

### 281 **3.2 Experimental temperature treatments**

282 Mean temperatures in the control and high pCO<sub>2</sub> treatments were 14.1 (± 0.35 sd) °C and in the  
283 high temperature and combination treatments the mean temperatures were 18.6 (± 0.42 sd) °C,  
284 with a mean temperature difference between the ambient and high temperature treatments of  
285 4.46 (± 0.42 sd) °C (Supplementary material, **Fig. S2 A & B**).

286

### 287 **3.3 Chlorophyll *a***

288 Mean Chl *a* in the experimental seawater at T0 was 1.64 (± 0.02 sd) mg m<sup>-3</sup> (**Fig. 3 A**). This  
289 decreased in all treatments between T0 to T7, to ~0.1 (± 0.09, 0.035 and 0.035 sd) mg m<sup>-3</sup> in the  
290 control, high pCO<sub>2</sub> and combination treatments, while in the high temperature treatment at T7  
291 Chl *a* was 0.46 mg m<sup>-3</sup> (± 0.29 sd) ( $z = 2.176, p < 0.05$ ). From T7 to T12 Chl *a* increased in all  
292 treatments which was highest in the combination (4.99 mg m<sup>-3</sup> ± 0.69 sd) and high pCO<sub>2</sub>  
293 treatments (3.83 mg m<sup>-3</sup> ± 0.43 sd). Overall, Chl *a* was significantly influenced by experimental  
294 time, independent of experimental treatments (**Table 1**). At T36 Chl *a* concentration in the  
295 combination treatment was higher (6.87 (± 0.58 sd) mg m<sup>-3</sup>) than all other treatments while the  
296 high temperature treatment concentration was higher (4.77 (± 0.44 sd) mg m<sup>-3</sup>) than the control  
297 and high pCO<sub>2</sub> treatment. Mean concentrations for the control and high pCO<sub>2</sub> treatment at T36  
298 were not significantly different at 3.30 (± 0.22 sd) and 3.46 (± 0.35 sd) mg m<sup>-3</sup> respectively  
299 (pairwise comparison  $t = 0.78, p = 0.858$ ).

### 300 3.4 Phytoplankton biomass

301 The starting biomass in all treatments was  $110.2 (\pm 5.7 \text{ sd}) \text{ mg C m}^{-3}$  (**Fig. 3 B**). The biomass was  
302 dominated by dinoflagellates ( $\sim 50\%$ ) with smaller contributions from nanophytoplankton  
303 ( $\sim 13\%$ ), cryptophytes ( $\sim 11\%$ ), diatoms ( $\sim 9\%$ ), coccolithophores ( $\sim 8\%$ ), *Synechococcus* ( $\sim 6\%$ )  
304 and picophytoplankton ( $\sim 3\%$ ). Total biomass was significantly influenced in all treatments over  
305 time (**Table 1**) and at T10, it was significantly higher in the high temperature treatment when  
306 biomass reached  $752 (\pm 106 \text{ sd}) \text{ mg C m}^{-3}$  ( $z = 2.769, p < 0.01$ ). Biomass was significantly higher  
307 in the elevated pCO<sub>2</sub> treatment (and interaction of time x high pCO<sub>2</sub>) (**Table 1**), reaching  $2481$   
308 ( $\pm 182.68 \text{ sd}) \text{ mg C m}^{-3}$  at T36, increasing more than 20-fold from T0 ( $z = 3.657, p < 0.001$ ). Total  
309 biomass in the high temperature treatment increased more than 15-fold to  $1735 (\pm 169.24 \text{ sd})$   
310  $\text{mg C m}^{-3}$  at T36 and was significantly higher than the combination treatment and ambient  
311 control ( $z = 2.744, p < 0.001$ ), which were  $525 (\pm 28.02 \text{ sd}) \text{ mg C m}^{-3}$  and  $378 (\pm 33.95 \text{ sd}) \text{ mg C}$   
312  $\text{m}^{-3}$ , respectively.

313 POC followed the same trends in all treatments between T0 and T36 (**Fig. 3 C**) and was in close  
314 range of the estimated biomass ( $R^2 = 0.914$ , **Fig. 3 D**). POC was significantly influenced by the  
315 interaction of time x high pCO<sub>2</sub> and time x high temperature (**Table 1**). At T36 POC was  
316 significantly higher in the high pCO<sub>2</sub> treatment ( $2086 \pm 155.19 \text{ sd mg m}^{-3}$ ) followed by the high  
317 temperature treatment ( $1594 \pm 162.24 \text{ sd mg m}^{-3}$ ) whereas a decline in POC was observed in  
318 the control and combination treatment. PON followed the same trend as POC over the course of  
319 the experiment, though it was only significantly influenced by the interaction between time x  
320 high pCO<sub>2</sub> (**Fig. 3 E, Table 1**). At T36 concentrations were  $147 (\pm 12.99 \text{ sd})$  and  $133 (\pm 15.59 \text{ sd})$   
321  $\text{mg m}^{-3}$  in the high pCO<sub>2</sub> and high temperature treatments respectively, while PON was  $57.75 (\pm$   
322  $13.07 \text{ sd}) \text{ mg m}^{-3}$  in the combination treatment and  $47.18 (\pm 9.32 \text{ sd}) \text{ mg m}^{-3}$  in the control.  
323 POC:PON ratios were significantly influenced by the interaction of time x high pCO<sub>2</sub> and time x  
324 high temperature (**Table 1**). The largest increase of 33 %, from 10.72 to  $14.26 \text{ mg m}^{-3} (\pm 1.73$   
325  $\text{sd})$  was in the high pCO<sub>2</sub> treatment, followed by an increase of 32 % to  $9.83 (\pm 1.82 \text{ sd}) \text{ mg m}^{-3}$   
326 in the combination treatment (lowest T0 starting value), and an increase of 17 % to  $12.09 (\pm$   
327  $2.14 \text{ sd}) \text{ mg m}^{-3}$  in the high temperature treatment. In contrast, the POC:PON ratio in the control  
328 declined by 20 % from T0 to T36, from 10.33 to  $8.26 (\pm 0.50 \text{ sd}) \text{ mg m}^{-3}$  (**Fig. 3 F**).

### 329 3.5 Community composition

330 From T0 to T24 the community shifted away from dominance of dinoflagellates in all  
331 treatments, followed by further regime shifts between T24 and T36 in the control and  
332 combination treatments. At T36 diatoms dominated the phytoplankton community biomass in  
333 the ambient control (**Fig. 4 A**), while the high temperature and high pCO<sub>2</sub> treatments exhibited

334 near mono-specific dominance of nanophytoplankton (**Figs. 4 B & C**). The most diverse  
335 community was in the combination treatment where dinoflagellates and *Synechococcus* became  
336 more prominent (**Fig. 4 D**).

337 Between T10 and T24 the community shifted to nanophytoplankton in all experimental  
338 treatments. This dominance was maintained to T36 in the high temperature and high pCO<sub>2</sub>  
339 treatments whereas in the ambient control and combination treatment, the community shifted  
340 away from nanophytoplankton (**Fig. 5 A**). Nanophytoplankton biomass was significantly higher  
341 in the high pCO<sub>2</sub> treatment (**Table 2**) with biomass reaching 2216 ( $\pm$  189.67 sd) mg C m<sup>-3</sup> at  
342 T36. This biomass was also high (though not significantly throughout the experiment until T36)  
343 in the high temperature treatment (T36: 1489 ( $\pm$  170.32 sd) mg C m<sup>-3</sup>,  $z = 1.695$ ,  $p = 0.09$ )  
344 compared to the control and combination treatments. In the combination treatment  
345 nanophytoplankton biomass was 238 ( $\pm$  14.16 sd) mg C m<sup>-3</sup> at T36 which was higher than the  
346 control, though not significantly ( $162 \pm 20.02$  sd mg C m<sup>-3</sup>). In addition to significant differences  
347 in nanophytoplankton biomass amongst the experimental treatments, treatment-specific  
348 differences in cell size were also observed. Larger nano-flagellates dominated the control (mean  
349 cell diameter of 6.34  $\mu$ m), smaller nano-flagellates dominated the high temperature and  
350 combination treatments (mean cell diameters of 3.61  $\mu$ m and 4.28  $\mu$ m) whereas *Phaeocystis* spp.  
351 dominated the high pCO<sub>2</sub> treatment (mean cell diameter 5.04  $\mu$ m) and was not observed in any  
352 other treatment (Supplementary material, **Fig. S3 A-D**).

353 At T0, diatom biomass was low and dominated by *Coscinodiscus wailessi* (48 %; 4.99 mg C m<sup>-3</sup>),  
354 *Pleurosigma* (25 %; 2.56 mg C m<sup>-3</sup>) and *Thalassiosira subtilis* (19 %; 1.94 mg C m<sup>-3</sup>). Small  
355 biomass contributions were made by *Navicula distans*, undetermined pennate diatoms and  
356 *Cylindrotheca closterium*. Biomass in the diatom group remained low from T0 to T24 but  
357 increased significantly through time in all treatments (**Table 2**), with the highest biomass in the  
358 high pCO<sub>2</sub> treatment ( $235 \pm 21.41$  sd mg C m<sup>-3</sup>, **Fig. 5 B**). The highest diatom contribution to  
359 total community biomass at T36 was in the ambient control (52 % of biomass;  $198 \pm 17.28$  sd  
360 mg C m<sup>-3</sup>). In both the high temperature and combination treatments diatom biomass was lower  
361 at T36 ( $151 \pm 10.94$  sd and  $124 \pm 19.16$  sd mg C m<sup>-3</sup>, respectively). In all treatments, diatom  
362 biomass shifted from the larger *C. Wailessii* to the smaller *C. closterium*, *N. distans*, *T. subtilis* and  
363 *Tropidoneis* spp., the relative contributions of which were treatment-specific. Overall *N. distans*  
364 dominated diatom biomass in all treatments at T36 (ambient control:  $112 \pm 24.86$  sd mg C m<sup>-3</sup>,  
365 56 % of biomass; high temperature:  $106 \pm 17.75$  sd mg C m<sup>-3</sup>, 70 % of biomass; high pCO<sub>2</sub>:  $152 \pm$   
366  $19.09$  sd mg C m<sup>-3</sup>, 61 % of biomass; and combination:  $111 \pm 20.97$  sd mg C m<sup>-3</sup>, 89 % of  
367 biomass; Supplementary material, **Fig. S4 A-D**).

368 The starting dinoflagellate community was dominated by *Gyrodinium spirale* (91 %; 49 mg C m<sup>-3</sup>)  
369 <sup>3</sup>), with smaller contributions from *Katodinium glaucum* (5 %; 2.76mg C m<sup>-3</sup>), *Prorocentrum*  
370 *cordatum* (3 %; 1.78 mg C m<sup>-3</sup>) and undetermined *Gymnodiniales* (1 %; 0.49 mg C m<sup>-3</sup>).  
371 Dinoflagellate biomass was significantly higher in the combination treatment (90 ± 16.98 sd mg  
372 C m<sup>-3</sup>, **Fig. 5 C, Table 2**) followed by the high temperature treatment (57 ± 6.87 sd mg C m<sup>-3</sup>,  
373 **Table 2**). There was no significant difference in dinoflagellate biomass between the high pCO<sub>2</sub>  
374 treatment and ambient control at T36 when biomass was low. In the combination treatment, the  
375 dinoflagellate biomass became dominated by *P. cordatum* which contributed 59 ± 12.95 sd mg C  
376 m<sup>-3</sup> (66 % of biomass in this group).

377 *Synechococcus* biomass was significantly higher in the combination treatment (reaching 59.9 ±  
378 4.30 sd mg C m<sup>-3</sup> at T36, **Fig. 5 D, Table 2**) followed by the high temperature treatment (30 ±  
379 5.98 sd mg C m<sup>-3</sup>, **Table 2**). In both the high pCO<sub>2</sub> treatment and control *Synechococcus* biomass  
380 was low (~7 mg C m<sup>-3</sup> in both treatments at T36), though an initial significant response to high  
381 pCO<sub>2</sub> was observed between T0 – T10 (**Table 2**). In all treatments and throughout the  
382 experiment, relative to the other phytoplankton groups, biomass of picophytoplankton (**Fig. 5**  
383 **E**), cryptophytes (**Fig. 5 F**) and coccolithophores (**Fig. 5 G**) remained low, though there was a  
384 slight increase in picophytoplankton in the combination treatment (11.26 ± 0.79 sd mg C m<sup>-3</sup>;  
385 **Table 2**).

### 386 **3.6 Chl *a* fluorescence-based photophysiology**

387 At T36, FRRf photosynthesis-irradiance (PE) parameters were strongly influenced by the  
388 experimental treatments. P<sup>B<sub>m</sub></sup> was significantly higher in the high pCO<sub>2</sub> treatment (18.93 mg C  
389 (mg Chl *a*)<sup>-1</sup> m<sup>-3</sup> h<sup>-1</sup>), followed by the high temperature treatment (9.58 mg C (mg Chl *a*)<sup>-1</sup> m<sup>-3</sup> h<sup>-1</sup>;  
390 **Fig. 6, Tables 3 & 4**). There was no significant difference in P<sup>B<sub>m</sub></sup> between the control and  
391 combination treatments (2.77 and 3.02 mg C (mg Chl *a*)<sup>-1</sup> m<sup>-3</sup> h<sup>-1</sup>). Light limited photosynthetic  
392 efficiency (α<sup>B</sup>) also followed the same trend and was significantly higher in the high pCO<sub>2</sub>  
393 treatment (0.13 mg C (mg Chl *a*)<sup>-1</sup> m<sup>-3</sup> h<sup>-1</sup> (μmol photon m<sup>-2</sup> s<sup>-1</sup>)<sup>-1</sup>) followed by the high  
394 temperature treatment (0.09 mg C (mg Chl *a*)<sup>-1</sup> m<sup>-3</sup> h<sup>-1</sup> (μmol photon m<sup>-2</sup> s<sup>-1</sup>)<sup>-1</sup>; **Tables 3 & 4**). α<sup>B</sup>  
395 was low in both the control and combination treatment (0.03 and 0.04 mg C (mg Chl *a*)<sup>-1</sup> m<sup>-3</sup> h<sup>-1</sup>  
396 (μmol photon m<sup>-2</sup> s<sup>-1</sup>)<sup>-1</sup>, respectively). The light saturation point of photosynthesis (*E<sub>k</sub>*) was  
397 significantly higher in the high pCO<sub>2</sub> treatment relative to all treatments (144.13 μmol photon  
398 m<sup>-2</sup> s<sup>-1</sup>), though significantly lower in the combination treatment relative to both the high pCO<sub>2</sub>  
399 and high temperature treatments (**Tables 3 & 4**).

## 400 **4. Discussion**

401 Individually, elevated temperature and pCO<sub>2</sub> resulted in the highest biomass and maximum  
402 photosynthetic rates (P<sup>B<sub>m</sub></sup>) at T36, when nanophytoplankton dominated. The interaction of  
403 these two factors had little effect on total biomass with values close to the ambient control, and  
404 no effect on P<sup>B<sub>m</sub></sup>. The combination treatment, however, exhibited the greatest diversity of  
405 phytoplankton functional groups with dinoflagellates and *Synechococcus* becoming dominant  
406 over time.

407 Elevated pCO<sub>2</sub> has been shown to enhance the growth and photosynthesis of some  
408 phytoplankton species which have active uptake systems for inorganic carbon (Giordano et al.,  
409 2005; Reinfelder, 2011). Elevated pCO<sub>2</sub> may therefore lead to lowered energetic costs of carbon  
410 assimilation in some species and a redistribution of the cellular energy budget to other  
411 processes (Tortell et al., 2002). In the present study, under elevated pCO<sub>2</sub> where the dominant  
412 group was nanophytoplankton, the community was dominated by the bloom-forming  
413 haptophyte *Phaeocystis* spp. Photosynthetic carbon fixation in *Phaeocystis* spp. is presently near  
414 saturation with respect to current levels of pCO<sub>2</sub> (Rost et al., 2003). Dominance of this spp.  
415 under elevated pCO<sub>2</sub> is likely to be due to variability in the C acquisition strategy, which could  
416 be advantageous over other species. The increased biomass and photosynthetic carbon fixation  
417 in this experimental under elevated pCO<sub>2</sub> is due to the community shift to *Phaeocystis* spp.. The  
418 increased biomass in the high temperature treatment may be attributed to enhanced enzymatic  
419 activities, since algal growth commonly increases with temperature until after an optimal range  
420 (Boyd et al., 2013; Goldman and Carpenter, 1974; Savage et al., 2004). Optimum growth  
421 temperatures for marine phytoplankton are often several degrees higher than environmental  
422 temperatures (Eppley, 1972; Thomas et al., 2012).

#### 423 **4.1 Chl *a***

424 Biomass in the control peaked at T25 followed by a decline to T36. Correlated with this, Chl *a*  
425 also peaked at T25 in the control and declined to 3.3 mg m<sup>-3</sup> by T27, remaining close to this  
426 value until T36. Biomass in the combination treatment peaked at T20 followed by decline to  
427 T36 whereas Chl *a* in this treatment declined from T20 to T25 followed by an increase at T27  
428 before further decline similar to the biomass. Chl *a* peaked in this treatment again at T36 (6.8  
429 mg m<sup>-3</sup>). We attribute the increase in Chl *a* between T25 – T27 (coincident with an overall  
430 biomass decrease) to lower species specific carbon:Chl *a* ratios as a result of the increase in  
431 dinoflagellates, *Synechococcus* and picophytoplankton biomass from T25. The decline in  
432 biomass under nutrient replete conditions in the combination treatment was probably due to  
433 slower species-specific growth rates when dinoflagellates dominated. This contrasts the results  
434 reported in comparable studies as Chl *a* is generally highly correlated with biomass, ( e.g. Feng

435 et al., 2009). Similar results were reported however by Hare et al., (2007) which indicates that  
436 Chl *a* may not always be a reliable proxy for biomass in mixed communities.

#### 437 **4.2 Biomass**

438 This study shows that the phytoplankton community response to elevated temperature and  
439 pCO<sub>2</sub> is highly variable. pCO<sub>2</sub> elevated to ~800 µatm induced higher community biomass, similar  
440 to the findings of Kim et al., (2006) and Riebesell et al., (2007), whereas in other natural  
441 community studies no CO<sub>2</sub> effect on biomass was observed (Delille et al., 2005; Maugendre et al.,  
442 2017; Paul et al., 2015). A ~4.5 °C increase in temperature also resulted in higher biomass at  
443 T36 in this study, similar to the findings of Feng et al., (2009) and Hare et al., (2007) though  
444 elevated temperature has previously reduced biomass of natural nanophytoplankton  
445 communities in the Western Baltic Sea and Arctic Ocean (Coello-Camba et al., 2014; Moustaka-  
446 Gouni et al., 2016). When elevated temperature and pCO<sub>2</sub> were combined, community biomass  
447 exhibited little response, similar to the findings of Gao et al., (2017), though an increase in  
448 biomass has also been reported (Calbet et al., 2014; Feng et al., 2009). Geographic location and  
449 season also play an important role in structuring the community and its response in terms of  
450 biomass to elevated temperature and pCO<sub>2</sub>. (Li et al., 2009; Morán et al., 2010). This may explain  
451 part of the variability in responses observed from studies on phytoplankton during different  
452 seasons and provinces.

#### 453 **4.3 Carbon:Nitrogen**

454 In agreement with others, the results of this experiment showed highest increases in C:N under  
455 elevated pCO<sub>2</sub> alone (Riebesell et al., 2007). C:N also increased under high temperature,  
456 consistent with the findings of Lomas and Glibert, (1999) and Taucher et al., (2015). It also  
457 increased when pCO<sub>2</sub> and temperature were elevated, albeit to a lesser degree, which was also  
458 observed by Calbet et al., (2014), but contrasts other studies that have observed C:N being  
459 unaffected by the combined influence of elevated pCO<sub>2</sub> and temperature (Deppeler and  
460 Davidson, 2017; Kim et al., 2006; C. Paul et al., 2015). C:N is a strong indicator of cellular protein  
461 content (Woods and Harrison, 2003) and increases under elevated pCO<sub>2</sub> and warming may lead  
462 to lowered nutritional value of phytoplankton which has implications for zooplankton  
463 reproduction and the biogeochemical cycling of nutrients.

#### 464 **4.4 Photosynthetic carbon fixation rates**

465 At T36, under elevated pCO<sub>2</sub> P<sup>B<sub>m</sub></sup> was > 6 times higher than in the control, which has also been  
466 reported by Riebesell et al., (2007) and Tortell et al., (2008). By contrast other observations on  
467 natural populations under elevated pCO<sub>2</sub> reported a reduction in P<sup>B<sub>m</sub></sup> (Feng et al., 2009; Hare et

468 al., 2007). Studies on laboratory cultures have shown that increases in temperature cause an  
469 increase photosynthetic rates (Feng et al., 2008; Fu et al., 2007; Hutchins et al., 2007), similar to  
470 what we observed in this study. In the combined pCO<sub>2</sub> and temperature treatment, we found no  
471 effect on P<sup>B</sup><sub>m</sub>, which has also been observed in experiments on natural populations (Coello-  
472 Camba and Agustí, 2016; Gao et al., 2017). This contrasts the findings of Feng et al., (2009) and  
473 Hare et al., (2007) who observed the highest P<sup>B</sup><sub>m</sub> when temperature and pCO<sub>2</sub> were elevated  
474 simultaneously. In this study, increases in  $\alpha^B$  and  $E_k$  under elevated pCO<sub>2</sub>, and a decrease in  
475 these parameters when elevated pCO<sub>2</sub> and temperature were combined also contrasts the  
476 trends reported by Feng et al., (2009).

477 Species specific photosynthetic rates have been demonstrated to decrease beyond a thermal  
478 optimum temperature of 20 °C (Raven and Geider, 1988) which can be modified through  
479 photoprotective rather than photosynthetic pigments (Kiefer and Mitchell, 1983). This may  
480 explain the difference in P<sup>B</sup><sub>m</sub> between the high pCO<sub>2</sub> and high temperature treatments (in  
481 addition to differences in nanophytoplankton community composition in relation to *Phaeocystis*  
482 spp. discussed above), as the experimental high temperature treatment in this study was ~4.5 °  
483 C higher the control.

484 There was no significant effect of combined elevated pCO<sub>2</sub> and temperature on P<sup>B</sup><sub>m</sub>, which was  
485 strongly influenced by taxonomic differences between the experimental treatments. Warming  
486 has been shown to lead to smaller cell sizes in nanophytoplankton (Atkinson et al., 2003; Peter  
487 and Sommer, 2012), which was observed in the combined treatment together with decreased  
488 nanophytoplankton biomass. Diatoms also shifted to smaller species with reduced biomass,  
489 while dinoflagellate and *Synechococcus* biomass increased at T36. Dinoflagellates are the only  
490 photoautotrophs with form II RuBisCO (Morse et al., 1995) which has the lowest  
491 carboxylation:oxygenation specificity factor among eukaryotic phytoplankton (Badger et al.,  
492 1998), which may give dinoflagellates a disadvantage in carbon fixation under present ambient  
493 pCO<sub>2</sub> levels. Phytoplankton growth rates are generally slower in surface waters with high pH  
494 ( $\geq 9$ ) resulting from photosynthetic removal of CO<sub>2</sub> by previous blooms, as is the case with  
495 dinoflagellates (Hansen, 2002; Hinga, 2002). Though growth under high pH provides indirect  
496 evidence that dinoflagellates possess CCMs, direct evidence is limited and points to the  
497 efficiency of CCMs in dinoflagellates as moderate in comparison to diatoms and some  
498 haptophytes (Reinfelder, 2011 and references therein). This may explain the lower P<sup>B</sup><sub>m</sub> in the  
499 combined treatment compared to elevated pCO<sub>2</sub> and temperature individually. We applied the  
500 same electron requirement parameter for carbon uptake across all treatments, though in nature  
501 and between species, there can be considerable variation in this parameter (e.g. 1.15 to 54.2 mol  
502 e<sup>-</sup> (mol C)<sup>-1</sup>; Lawrenz et al., 2013) which can co-vary with temperature, nutrients, Chl  $a$ ,

503 irradiance and community structure. Better measurement techniques at quantifying this  
504 variability are necessary in the future.

#### 505 **4.5 Community composition**

506 Phytoplankton community structure changes were observed, with a shift from dinoflagellates to  
507 nanophytoplankton which was most pronounced under single treatments of elevated  
508 temperature and pCO<sub>2</sub>. Amongst the nanophytoplankton, a distinct size shift to smaller cells was  
509 observed in the high temperature and combination treatments, while in the high pCO<sub>2</sub>  
510 treatment *Phaeocystis* spp. dominated. Under combined pCO<sub>2</sub> and temperature from T24  
511 onwards however, dinoflagellate and *Synechococcus* biomass increased and nanophytoplankton  
512 biomass decreased. An increase in pico- and nanophytoplankton has previously been reported  
513 in natural communities under elevated pCO<sub>2</sub> (Bermúdez et al., 2016; Boras et al., 2016;  
514 Brussaard et al., 2013; Engel et al., 2008) while no effect on these size classes has been observed  
515 in other studies (Calbet et al., 2014; Paulino et al., 2007). Moustaka-Gouni et al., (2016) also  
516 found no CO<sub>2</sub> effect on natural nanophytoplankton communities but increased temperature  
517 reduced the biomass of this group. Kim et al., (2006) observed a shift from nanophytoplankton  
518 to diatoms under elevated pCO<sub>2</sub> alone while a shift from diatoms to nanophytoplankton under  
519 combined elevated pCO<sub>2</sub> and temperature has been reported (Hare et al., 2007). A variable  
520 response in *Phaeocystis* spp. to elevated pCO<sub>2</sub> has also been reported with increased growth  
521 (Chen et al., 2014; Keys et al., 2017), no effect (Thoisen et al., 2015) and decreased growth  
522 (Hoogstraten et al., 2012) observed. *Phaeocystis* spp. can outcompete other phytoplankton and  
523 form massive blooms (up to 10 g C m<sup>-3</sup>) with impacts on food webs, global biogeochemical  
524 cycles and climate regulation (Schoemann et al., 2005). While not a toxic algal species,  
525 *Phaeocystis* spp. are considered a harmful algal bloom (HAB) species when biomass reaches  
526 sufficient concentrations to cause anoxia through the production of mucus foam which can clog  
527 the feeding apparatus of zooplankton and fish (Eilertsen & Raa, 1995).

528 Recently published studies on the response of diatoms to elevated pCO<sub>2</sub> and temperature vary  
529 greatly. For example, Taucher et al., (2015) showed that *Thalassiosira weissflogii* incubated at  
530 1000 µatm pCO<sub>2</sub> increased growth by 8 % while for *Dactyliosolen fragilissimus*, growth  
531 increased by 39 %; temperature elevated by + 5°C also had a stimulating effect on *T. weissflogii*  
532 but inhibited the growth rate of *D. fragilissimus*; and when the treatments were combined  
533 growth was enhanced in *T. weissflogii* but reduced in *D. fragilissimus*. In our study, elevated pCO<sub>2</sub>  
534 increased biomass in diatoms (time dependent), but elevated temperature and the combination  
535 of these factors reduced the signal of this response. A distinct size-shift in diatom species was  
536 observed in all treatments, from the larger *Coscinodiscus* spp., *Pleurosigma* and *Thalassiosira*  
537 *subtilis* to the smaller *Navicula distans*. This was most pronounced in the combination treatment



538 where *N. distans* formed 89 % of diatom biomass. *Navicula* spp. previously exhibited a  
539 differential response to both elevated temperature and pCO<sub>2</sub>. At + 4.5 °C and 960 ppm CO<sub>2</sub>  
540 Torstensson et al., (2012) observed no synergistic effects on the benthic *Navicula directa*.  
541 Elevated temperature increased growth rates by 43 % while a reduction of 5 % was observed  
542 under elevated CO<sub>2</sub>. No effects on growth were detected at pH ranging from 8 – 7.4 units in  
543 *Navicula* spp. (Thoisen et al., 2015), while there was a significant increase in growth in *N.*  
544 *distans* along a CO<sub>2</sub> gradient at a shallow cold-water vent system (Baragi et al., 2015).

545 *Synechococcus* grown under pCO<sub>2</sub> elevated to 750 ppm and temperature elevated by 4 °C  
546 resulted in increased growth and a 4-fold increase in P<sup>B<sub>m</sub></sup> (Fu et al., 2007) which is similar to the  
547 results of the present study.

548 The combination of elevated temperature and pCO<sub>2</sub> significantly increased dinoflagellate  
549 biomass to 17 % of total biomass. This was due to *P. cordatum* which increased biomass by  
550 more than 30-fold from T0 to T30 (66 % of dinoflagellate biomass in this treatment). Despite  
551 the global increase in the frequency of HABs few studies have focussed on the response of  
552 dinoflagellates to elevated pCO<sub>2</sub> and temperature. In laboratory studies at 1000 ppm CO<sub>2</sub>,  
553 growth rates of the HAB species *Karenia brevis* increased by 46 %, at 1000 ppm CO<sub>2</sub> and + 5 °C  
554 temperature it's growth increased by 30 % but was reduced under elevated temperature alone  
555 (Errera et al., 2014). A combined increase in pCO<sub>2</sub> and temperature enhanced both the growth  
556 and P<sup>B<sub>m</sub></sup> in the dinoflagellate *Heterosigma akashiwo*, whereas in contrast to the present findings,  
557 only pCO<sub>2</sub> alone enhanced these parameters in *P. cordatum* (Fu et al., 2008).

## 558 **5. Implications**

559 Increased biomass, P<sup>B<sub>m</sub></sup> and a community shift to nanophytoplankton under individual increases  
560 in temperature and pCO<sub>2</sub> suggests a potential positive feedback on atmospheric CO<sub>2</sub>, whereby  
561 more CO<sub>2</sub> is removed from the ocean, and hence from the atmosphere through an increase in  
562 photosynthesis. The selection of *Phaeocystis* spp. under elevated pCO<sub>2</sub> indicates the potential for  
563 negative impacts on ecosystem function and food web structure due to the formation of hypoxic  
564 zones, inhibitory feeding effects and lowered fecundity in many copepods associated with this  
565 species (Schoemann et al., 2005; Verity et al., 2007). While more CO<sub>2</sub> is fixed, selection for  
566 nanophytoplankton in both of these treatments however, may result in reduced carbon  
567 sequestration due to slower sinking rates of the smaller phytoplankton cells (Bopp et al., 2001;  
568 Laws et al., 2000). When temperature and pCO<sub>2</sub> were elevated simultaneously, community  
569 biomass showed little response and no effects on P<sup>B<sub>m</sub></sup> were observed. This suggests a negative  
570 feedback on atmospheric CO<sub>2</sub> and climate warming due to reduced drawdown of CO<sub>2</sub> in future  
571 warmer high CO<sub>2</sub> oceans. Additionally, combined elevated pCO<sub>2</sub> and temperature significantly

572 modified taxonomic composition, by reducing diatom biomass relative to the control with an  
573 increase in dinoflagellate biomass dominated by the HAB species, *P. cordatum*. This has  
574 implications for fisheries, ecosystem function and human health.

## 575 6. Conclusion

576 These experimental results provide new evidence that increases in pCO<sub>2</sub> coupled with rising sea  
577 temperatures may have antagonistic effects on the autumn phytoplankton community in the  
578 WEC. Under future global change scenarios, the size range and biomass of diatoms may be  
579 reduced with increased dinoflagellate biomass and the selection of HAB species. The  
580 experimental simulations of year 2100 temperature and pCO<sub>2</sub> demonstrate that the effects of  
581 warming can be offset by elevated pCO<sub>2</sub> potentially reducing coastal phytoplankton productivity  
582 and significantly altering the community structure, and in turn these shifts will have  
583 consequences on carbon biogeochemical cycling in the WEC.

584 **Data availability:** Experimental data used for analysis will be made available (DOI will be  
585 created)

586 **Author contributions:** Matthew Keys collected, measured, processed and analysed the data and  
587 prepared the figures. Drs Gavin Tilstone and Helen Findlay conceived, directed and sought the  
588 necessary funds to support the research. Matthew Keys and Dr Gavin Tilstone wrote the paper  
589 with input from Claire Widdicombe and Professor Tracy Lawson. Claire Widdicombe supervised  
590 and advised on phytoplankton taxonomic classifications.

591 **Competing interests:** The authors declare that they have no conflict of interest.

592 **Acknowledgements:** G.H.T, H.S.F. and C.E.W were supported by the UK Natural Environment  
593 Research Council's (NERC) National Capability – The Western English Channel Observatory  
594 (WCO). C.E.W was also partly funded by the NERC and Department for Environment, Food and  
595 Rural Affairs, Marine Ecosystems Research Program (Grant no. NE/L003279/1). M.K. was  
596 supported by a NERC PhD studentship (grant No. NE/L50189X/1). We thank Glen Tarran for his  
597 training, help and assistance with flow cytometry, The National Earth Observation Data Archive  
598 and Analysis Service UK (NEODAAS) for providing the MODIS image used in Fig 1. and the crew  
599 of RV Plymouth Quest for their helpful assistance during field sampling.

## 600 References

601 Alley, D., Berntsen, T., Bindoff, N. L., Chen, Z. L., Chidthaisong, A., Friedlingstein, P., Gregory, J., G.,  
602 H., Heimann, M., Hewitson, B., Hoskins, B., Joos, F., Jouzel, J., Kattsov, V., Lohmann, U., Manning, M.,

603 Matsuno, T., Molina, M., Nicholls, N., Overpeck, J., Qin, D.H., Raga, G. Ramaswamy, V., Ren, J.W.,  
604 Rusticucci, M., Solomon, S. and Somerville, R., Stocker, T.F., Stott, P., Stouffer, R.J. Whetton, P.,  
605 Wood, R.A. & Wratt, D.: Climate Change 2007. The Physical Science basis: Summary for  
606 policymakers. Contribution of Working Group I to the Fourth Assessment Report of the  
607 Intergovernmental Panel on Climate Change.

608 Atkinson, D., Ciotti, B. J. and Montagnes, D. J. S.: Protists decrease in size linearly with  
609 temperature: ca. 2.5% C<sup>-1</sup>, Proc. R. Soc. B Biol. Sci., 270(1533), 2605–2611,  
610 doi:10.1098/rspb.2003.2538, 2003.

611 Badger, M. R., Andrews, T. J., Whitney, S. M., Ludwig, M., Yellowlees, D. C., Leggat, W. and Price, G.  
612 D.: The diversity and coevolution of Rubisco , plastids , pyrenoids , and chloroplast-based CO<sub>2</sub> -  
613 concentrating mechanisms in algae 1, Can. J. Bot., (76), 1052–1071, 1998.

614 Baragi, L. V., Khandeparker, L. and Anil, A. C.: Influence of elevated temperature and pCO<sub>2</sub> on the  
615 marine periphytic diatom *Navicula distans* and its associated organisms in culture,  
616 Hydrobiologia, 762(1), 127–142, doi:10.1007/s10750-015-2343-9, 2015.

617 Barnes, M. K., Tilstone, G. H., Smyth, T. J., Widdicombe, C. E., Gloël, J., Robinson, C., Kaiser, J. and  
618 Suggett, D. J.: Drivers and effects of *Karenia mikimotoi* blooms in the western English Channel,  
619 Prog. Oceanogr., 137, 456–469, doi:10.1016/j.pocean.2015.04.018, 2015.

620 Beardall, J., Stojkovic., S. and Larsen., S.: Living in a high CO<sub>2</sub> world: impacts of global climate  
621 change on marine phytoplankton, Plant Ecol. Divers., 2(2), 191–205,  
622 doi:10.1080/17550870903271363, 2009.

623 Bermúdez, J. R., Riebesell, U., Larsen, A. and Winder, M.: Ocean acidification reduces transfer of  
624 essential biomolecules in a natural plankton community, Sci. Rep., 6(1), 27749,  
625 doi:10.1038/srep27749, 2016.

626 Booth, B. C.: Size classes and major taxonomic groups of phytoplankton at two locations in the  
627 subarctic pacific ocean in May and August, 1984, Mar. Biol., 97(2), 275–286,  
628 doi:10.1007/BF00391313, 1988.

629 Bopp, L. ., Monfray, P. ., Aumont, O. ., Dufresne, J.-L. ., Le Treut, H. ., Madec, G. ., Terray, L. . and  
630 Orr, J. C. .: Potential impact of climate change on marine export production, Global Biogeochem.  
631 Cycles, 15(1), 81–99, doi:10.1029/1999GB001256, 2001.

632 Boras, J. A., Borrull, E., Cardelu, C., Cros, L., Gomes, A., Sala, M. M., Aparicio, F. L., Balague, V.,  
633 Mestre, M., Movilla, J., Sarmiento, H., Va, E. and Lo, A.: Contrasting effects of ocean acidification on  
634 the microbial food web under different trophic conditions, ICES J. Mar. Sci., 73(73 (3)), 670–679,

635 2016.

636 Boyd, P. W. and Doney, S. C.: Modelling regional responses by marine pelagic ecosystems to  
637 global climate change, *Geophys. Res. Lett.*, 29(16), 1–4, 2002.

638 Boyd, P. W., Rynearson, T. A., Armstrong, E. A., Fu, F., Hayashi, K., Hu, Z., Hutchins, D. A., Kudela,  
639 R. M., Litchman, E., Mulholland, M. R., Passow, U., Strzepek, R. F., Whittaker, K. A., Yu, E. and  
640 Thomas, M. K.: Marine Phytoplankton Temperature versus Growth Responses from Polar to  
641 Tropical Waters - Outcome of a Scientific Community-Wide Study, *PLoS One*, 8(5),  
642 doi:10.1371/journal.pone.0063091, 2013.

643 Brussaard, C. P. D., Noordeloos, A. A. M., Witte, H., Collenteur, M. C. J., Schulz, K., Ludwig, A. and  
644 Riebesell, U.: Arctic microbial community dynamics influenced by elevated CO<sub>2</sub> levels,  
645 *Biogeosciences*, 10(2), 719–731, doi:10.5194/bg-10-719-2013, 2013.

646 Calbet, A., Sazhin, A. F., Nejstgaard, J. C., Berger, S. A, Tait, Z. S., Olmos, L., Sousoni, D., Isari, S.,  
647 Martínez, R. A, Bouquet, J.-M., Thompson, E. M., Båmstedt, U. and Jakobsen, H. H.: Future climate  
648 scenarios for a coastal productive planktonic food web resulting in microplankton phenology  
649 changes and decreased trophic transfer efficiency., *PLoS One*, 9(4), e94388,  
650 doi:10.1371/journal.pone.0094388, 2014.

651 Chen, S., Beardall, J. and Gao, K.: A red tide alga grown under ocean acidification upregulates its  
652 tolerance to lower pH by increasing its photophysiological functions, *Biogeosciences*, 11, 4829–  
653 4837, doi:10.5194/bg-11-4829-2014, 2014.

654 Coello-Camba, A. and Agustí, S.: Acidification counteracts negative effects of warming on diatom  
655 silicification, *Biogeosciences Discuss.*, 30(October), 1–19, doi:10.5194/bg-2016-424, 2016.

656 Coello-Camba, A., Agustí, S., Holding, J., Arrieta, J. M. and Duarte, C. M.: Interactive effect of  
657 temperature and CO<sub>2</sub> increase in Arctic phytoplankton, *Front. Mar. Sci.*, 1(October), 1–10,  
658 doi:10.3389/fmars.2014.00049, 2014.

659 Delille, B., Harlay, J., Zondervan, I., Jacquet, S., Chou, L., Wollast, R., Bellerby, R. G. J.,  
660 Frankignoulle, M., Borges, A. V., Riebesell, U. and Gattuso, J.-P.: Response of primary production  
661 and calcification to changes of p CO<sub>2</sub> during experimental blooms of the coccolithophorid  
662 *Emiliana huxleyi*, *Global Biogeochem. Cycles*, 19(2), n/a-n/a, doi:10.1029/2004GB002318,  
663 2005.

664 Deppeler, S. L. and Davidson, A. T.: Southern Ocean Phytoplankton in a Changing Climate, *Front.*  
665 *Mar. Sci.*, 4(February), doi:10.3389/fmars.2017.00040, 2017.

666 Dickson, A. G. and Millero, F. J.: A comparison of the equilibrium constants for the dissociation of

667 carbonic acid in seawater media, *Deep Sea Res. Part I Oceanogr. Res. Pap.*, 34(111), 1733–1743,  
668 1987.

669 Dunne, J. P.: A roadmap on ecosystem change, *Nat. Clim. Chang.*, 5, 20 [online] Available from:  
670 <http://dx.doi.org/10.1038/nclimate2480>, 2014.

671 Edwards, M., Johns, D., Leterme, S. C., Svendsen, E. and Richardson, A. J.: Regional climate change  
672 and harmful algal blooms in the northeast Atlantic, *Limnol. Oceanogr.*, 51(2), 820–829,  
673 doi:10.4319/lo.2006.51.2.0820, 2006.

674 Eilertsen, H. and Raa, J.: Toxins in seawater produced by a common phytoplankter : *Phaeocystis*  
675 *pouchetii*, *J. Mar. Biotechnol.*, 3(1), 115–119 [online] Available from:  
676 <http://ci.nii.ac.jp/naid/10002209414/en/> (Accessed 28 January 2016), 1995.

677 Engel, A., Schulz, K. G., Riebesell, U., Bellerby, R., Delille, B. and Schartau, M.: Effects of CO<sub>2</sub> on  
678 particle size distribution and phytoplankton abundance during a mesocosm bloom experiment  
679 (PeECE II), *Biogeosciences*, 5, 509–521, doi:10.5194/bgd-4-4101-2007, 2008.

680 Eppley, R. W.: Temperature and phytoplankton growth in the sea, *Fish. Bull.*, 70(4), 1063–1085,  
681 1972.

682 Errera, R. M., Yvon-Lewis, S., Kessler, J. D. and Campbell, L.: Responses of the dinoflagellate  
683 *Karenia brevis* to climate change: pCO<sub>2</sub> and sea surface temperatures, *Harmful Algae*, 37, 110–  
684 116, doi:10.1016/j.hal.2014.05.012, 2014.

685 Feng, Y., Warner, M. E., Zhang, Y., Sun, J., Fu, F.-X., Rose, J. M. and Hutchins, D. A.: Interactive  
686 effects of increased pCO<sub>2</sub>, temperature and irradiance on the marine coccolithophore *Emiliania*  
687 *huxleyi* (Prymnesiophyceae), *Eur. J. Phycol.*, 43(1), 87–98, doi:10.1080/09670260701664674,  
688 2008.

689 Feng, Y., Hare, C., Leblanc, K., Rose, J., Zhang, Y., DiTullio, G., Lee, P., Wilhelm, S., Rowe, J., Sun, J.,  
690 Nemcek, N., Gueguen, C., Passow, U., Benner, I., Brown, C. and Hutchins, D.: Effects of increased  
691 pCO<sub>2</sub> and temperature on the North Atlantic spring bloom. I. The phytoplankton community  
692 and biogeochemical response, *Mar. Ecol. Prog. Ser.*, 388, 13–25, doi:10.3354/meps08133, 2009.

693 Fu, F.-X., Warner, M. E., Zhang, Y., Feng, Y. and Hutchins, D. A.: Effects of Increased Temperature  
694 and CO<sub>2</sub> on Photosynthesis, Growth, and Elemental Ratios in Marine *Synechococcus* and  
695 *Prochlorococcus* (Cyanobacteria), *J. Phycol.*, 43(3), 485–496, doi:10.1111/j.1529-  
696 8817.2007.00355.x, 2007a.

697 Fu, F.-X., Zhang, Y., Warner, M. E., Feng, Y., Sun, J. and Hutchins, D. A.: A comparison of future  
698 increased CO<sub>2</sub> and temperature effects on sympatric *Heterosigma akashiwo* and *Prorocentrum*

699 *minimum*, Harmful Algae, 7(1), 76–90, doi:10.1016/j.hal.2007.05.006, 2008.

700 Gao, G., Jin, P., Liu, N., Li, F., Tong, S., Hutchins, D. A. and Gao, K.: The acclimation process of  
701 phytoplankton biomass, carbon fixation and respiration to the combined effects of elevated  
702 temperature and pCO<sub>2</sub> in the northern South China Sea, Mar. Pollut. Bull., 118(1–2), 213–220,  
703 doi:10.1016/j.marpolbul.2017.02.063, 2017.

704 Giordano, M., Beardall, J. and Raven, J. A: CO<sub>2</sub> concentrating mechanisms in algae: mechanisms,  
705 environmental modulation, and evolution., Annu. Rev. Plant Biol., 56(January), 99–131,  
706 doi:10.1146/annurev.arplant.56.032604.144052, 2005.

707 Goldman, J. and Carpenter, E.: A kinetic approach to the effect of temperature on algal growth,  
708 Limnol. Oceanogr., 19(5), 756–766, doi:10.4319/lo.1974.19.5.0756, 1974.

709 Hansen, P.: Effect of high pH on the growth and survival of marine phytoplankton: implications  
710 for species succession, Aquat. Microb. Ecol., 28, 279–288, doi:10.3354/ame028279, 2002.

711 Hare, C., Leblanc, K., DiTullio, G., Kudela, R., Zhang, Y., Lee, P., Riseman, S. and Hutchins, D.:  
712 Consequences of increased temperature and CO<sub>2</sub> for phytoplankton community structure in the  
713 Bering Sea, Mar. Ecol. Prog. Ser., 352, 9–16, doi:10.3354/meps07182, 2007a.

714 Hinga, K. R.: Effects of pH on coastal marine phytoplankton, Mar. Ecol. Prog. Ser., 238, 281–300,  
715 2002.

716 Hoogstraten, A., Peters, M., Timmermans, K. R. and De Baar, H. J. W.: Combined effects of  
717 inorganic carbon and light on *Phaeocystis globosa* Scherffel (Prymnesiophyceae),  
718 Biogeosciences, 9(5), 1885–1896, doi:10.5194/bg-9-1885-2012, 2012.

719 Hutchins, D. A., Fu, F.-X., Zhang, Y., Warner, M. E., Feng, Y., Portune, K., Bernhardt, P. W. and  
720 Mulholland, M. R.: CO<sub>2</sub> control of *Trichodesmium* N<sub>2</sub> fixation, photosynthesis, growth rates, and  
721 elemental ratios: Implications for past, present, and future ocean biogeochemistry, Limnol.  
722 Oceanogr., 52(4), 1293–1304, doi:10.4319/lo.2007.52.4.1293, 2007.

723 IPCC: Climate Change 2013: The Physical Science Basis. Contribution of Working Group I to the  
724 Fifth Assessment Report of the Intergovernmental Panel on Climate Change, Intergov. Panel  
725 Clim. Chang. Work. Gr. I Contrib. to IPCC Fifth Assess. Rep. (AR5)(Cambridge Univ Press. New  
726 York), 1535, doi:10.1029/2000JD000115, 2013.

727 Keys, M.: “Effects of future CO<sub>2</sub> and temperature regimes on phytoplankton community  
728 composition, biomass and photosynthetic rates in the Western English Channel”, PhD thesis.,  
729 University of Essex, United Kingdom., 2017.

730 Keys, M., Tilstone, G., Findlay, H. S., Widdicombe, C. E. and Lawson, T.: Effects of elevated CO<sub>2</sub> on  
731 phytoplankton community biomass and species composition during a spring *Phaeocystis* spp.  
732 bloom in the western English Channel, *Harmful Algae*, 67, 92–106,  
733 doi:10.1016/j.hal.2017.06.005, 2017.

734 Kiefer, D. A. and Mitchell, B. G.: A simple steady state description of phytoplankton growth based  
735 on absorption cross section and quantum efficiency, *Limnol. Oceanogr.*, 28(4), 770–776,  
736 doi:10.4319/lo.1983.28.4.0770, 1983.

737 Kim, J.-M., Lee, K., Shin, K., Kang, J.-H., Lee, H.-W., Kim, M., Jang, P.-G. and Jang, M.-C.: The effect of  
738 seawater CO<sub>2</sub> concentration on growth of a natural phytoplankton assemblage in a controlled  
739 mesocosm experiment, *Limnol. Oceanogr.*, 51(4), 1629–1636, doi:10.4319/lo.2006.51.4.1629,  
740 2006a.

741 Kitidis, V., Hardman-mountford, N. J., Litt, E., Brown, I., Cummings, D., Hartman, S., Hydes, D.,  
742 Fishwick, J. R., Harris, C., Martinez-vicente, V., Woodward, E. M. S. and Smyth, T. J.: Seasonal  
743 dynamics of the carbonate system in the Western English Channel, *Cont. Shelf Res.*, 42, 2–12,  
744 2012.

745 Kolber, Z. S., Prášil, O. and Falkowski, P. G.: Measurements of variable chlorophyll fluorescence  
746 using fast repetition rate techniques: Defining methodology and experimental protocols,  
747 *Biochim. Biophys. Acta - Bioenerg.*, 1367(1–3), 88–106, doi:10.1016/S0005-2728(98)00135-2,  
748 1998.

749 Lawrenz, E., Silsbe, G., Capuzzo, E., Ylöstalo, P., Forster, R. M., Simis, S. G. H., Prášil, O.,  
750 Kromkamp, J. C., Hickman, A. E., Moore, C. M., Forget, M. H., Geider, R. J. and Suggett, D. J.:  
751 Predicting the Electron Requirement for Carbon Fixation in Seas and Oceans, *PLoS One*, 8(3),  
752 doi:10.1371/journal.pone.0058137, 2013.

753 Laws, E. A., Falkowski, P. G., Smith, W. O., Ducklow, H. W. and McCarthy, J. J.: Temperature effects  
754 on export production in the open ocean, *Global Biogeochem. Cycles*, 14(4), 1231–1246,  
755 doi:10.1029/1999GB001229, 2000.

756 Li, W. K. W., McLaughlin, F. A., Lovejoy, C. and Carmack, E. C.: Smallest Algae Thrive As the Arctic  
757 Ocean Freshens, *Science* (80-. ), 326(5952), 539–539, doi:10.1126/science.1179798, 2009.

758 Lomas, M. W. and Glibert, P. M.: Interactions between NH<sub>4</sub><sup>+</sup> and NO<sub>3</sub><sup>-</sup> uptake and assimilation:  
759 Comparison of diatoms and dinoflagellates at several growth temperatures, *Mar. Biol.*, 133(3),  
760 541–551, doi:10.1007/s002270050494, 1999.

761 Love, B. A., Olson, M. B. and Wuori, T.: Technical Note: A minimally-invasive experimental

762 system for pCO<sub>2</sub> manipulation in plankton cultures using passive gas exchange (Atmospheric  
763 Carbon Control Simulator), *Biogeosciences Discuss.*, (December), 1–19, doi:10.5194/bg-2016-  
764 502, 2016.

765 Matear, R. J. and Lenton, A.: Carbon–climate feedbacks accelerate ocean acidification,  
766 *Biogeosciences*, 15(6), 1721–1732, doi:10.5194/bg-15-1721-2018, 2018.

767 Maugendre, L., Gattuso, J. P., Poulton, A. J., Dellisanti, W., Gaubert, M., Guieu, C. and Gazeau, F.: No  
768 detectable effect of ocean acidification on plankton metabolism in the NW oligotrophic  
769 Mediterranean Sea: Results from two mesocosm studies, *Estuar. Coast. Shelf Sci.*, 186, 89–99,  
770 doi:10.1016/j.ecss.2015.03.009, 2017.

771 Mehrbach, C., Culberson, C. H., Hawley, J. E. and Pytkowicz, R. M.: Measurement of the Apparent  
772 Dissociation Constants of Carbonic Acid in Seawater at Atmospheric Pressure, *Limnol.*  
773 *Oceanogr.*, 18(1932), 897–907, 1973.

774 Menden-Deuer, S. and Lessard, E. J.: Carbon to volume relationships for dinoflagellates, diatoms,  
775 and other protist plankton, *Limnol. Oceanogr.*, 45(3), 569–579, doi:10.4319/lo.2000.45.3.0569,  
776 2000.

777 Morán, X. A. G., López-Urrutia, Á., Calvo-Díaz, A. and Li, W. K. W.: Increasing importance of small  
778 phytoplankton in a warmer ocean, *Glob. Chang. Biol.*, 16(3), 1137–1144, doi:10.1111/j.1365-  
779 2486.2009.01960.x, 2010.

780 Morse, D., Salois, P., Markovic, P. and Hastings, J. W.: A nuclear-encoded form II RuBisCO in  
781 dinoflagellates., *Science*, 268(5217), 1622–1624, doi:10.1126/science.7777861, 1995.

782 Moustaka-Gouni, M., Kormas, K. A., Scotti, M., Vardaka, E. and Sommer, U.: Warming and  
783 Acidification Effects on Planktonic Heterotrophic Pico- and Nanoflagellates in a Mesocosm  
784 Experiment, *Protist*, 167(4), 389–410, doi:10.1016/j.protis.2016.06.004, 2016.

785 Oxborough, K., Moore, C. M., Suggett, D. J., Lawson, T., Chan, H. G. and Geider, R. J.: Direct  
786 estimation of functional PSII reaction center concentration and PSII electron flux on a volume  
787 basis: a new approach to the analysis of Fast Repetition Rate fluorometry (FRRf) data, *Limnol.*  
788 *Oceanogr. Methods*, 10, 142–154, doi:10.4319/lom.2012.10.142, 2012.

789 Paul, C., Matthiessen, B. and Sommer, U.: Warming, but not enhanced CO<sub>2</sub> concentration,  
790 quantitatively and qualitatively affects phytoplankton biomass, *Mar. Ecol. Prog. Ser.*, 528, 39–51,  
791 doi:10.3354/meps11264, 2015.

792 Paulino, A. I., Egge, J. K. and Larsen, a.: Effects of increased atmospheric CO<sub>2</sub> on small and  
793 intermediate sized osmotrophs during a nutrient induced phytoplankton bloom, *Biogeosciences*



794 Discuss., 4(6), 4173–4195, doi:10.5194/bgd-4-4173-2007, 2007.

795 Peter, K. H. and Sommer, U.: Phytoplankton Cell Size: Intra- and Interspecific Effects of Warming  
796 and Grazing, PLoS One, 7(11), doi:10.1371/journal.pone.0049632, 2012.

797 Pierrot, D., Lewis, E. and Wallace, D. W. R.: MS Excel program developed for CO<sub>2</sub> system  
798 calculations, ORNL/CDIAC-105a. Carbon Dioxide Inf. Anal. Center, Oak Ridge Natl. Lab. US Dep.  
799 Energy, Oak Ridge, Tennessee, 2006.

800 Raupach, M. R., Marland, G., Ciais, P., Le Quéré, C., Canadell, J. G., Klepper, G. and Field, C. B.:  
801 Global and regional drivers of accelerating CO<sub>2</sub> emissions., Proc. Natl. Acad. Sci. U. S. A., 104(24),  
802 10288–93, doi:10.1073/pnas.0700609104, 2007.

803 Raven. J., Caldeira. K., Elderfield. H., H.-G. and others: Ocean acidification due to increasing  
804 atmospheric carbon dioxide, R. Soc., (June), 2005.

805 Raven, J. A. and Geider, R. J.: Temperature and algal growth, New Phytol., 110(4), 441–461,  
806 doi:10.1111/j.1469-8137.1988.tb00282.x, 1988.

807 Reinfelder, J. R.: Carbon Concentrating Mechanisms in Eukaryotic Marine Phytoplankton, Ann.  
808 Rev. Mar. Sci., 3(1), 291–315, doi:10.1146/annurev-marine-120709-142720, 2011.

809 Riebesell, U.: Effects of CO<sub>2</sub> Enrichment on Marine Phytoplankton, J. Oceanogr., 60(4), 719–729,  
810 doi:10.1007/s10872-004-5764-z, 2004.

811 Riebesell, U., Schulz, K. G., Bellerby, R. G. J., Botros, M., Fritsche, P., Meyerhöfer, M., Neill, C.,  
812 Nondal, G., Oschlies, a, Wohlers, J. and Zöllner, E.: Enhanced biological carbon consumption in a  
813 high CO<sub>2</sub> ocean., Nature, 450(7169), 545–8, doi:10.1038/nature06267, 2007.

814 Riebesell, U., Fabry, V. J., Hansson, L. and Gattuso, J.-P.: Guide to best practices for ocean  
815 acidification, edited by L. H. and J. -P. G. L. U. Riebesell, V. J. Fabry, Publications Office Of The  
816 European Union., 2010.

817 Rost, B., Riebesell, U., Burkhardt, S. and Su, D.: Carbon acquisition of bloom-forming marine  
818 phytoplankton, Limnol. Oceanogr., 48(1), 55–67, 2003.

819 Savage, V. M., Gillooly, J. F., Brown, J. H., West, G. B. and Charnov, E. L.: Effects of Body Size and  
820 Temperature on Population Growth, Am. Nat., 163(3), 429–441, doi:10.1086/381872, 2004.

821 Schoemann, V., Becquevort, S., Stefels, J., Rousseau, V. and Lancelot, C.: *Phaeocystis* blooms in the  
822 global ocean and their controlling mechanisms: a review, J. Sea Res., 53(1–2), 43–66,  
823 doi:10.1016/j.seares.2004.01.008, 2005.

824 Schulz, K. G., Ramos, J. B., Zeebe, R. E. and Riebesell, U.: Biogeosciences CO<sub>2</sub> perturbation

825 experiments : similarities and differences between dissolved inorganic carbon and total  
826 alkalinity manipulations, *Biogeosciences*, 6, 2145–2153, 2009.

827 Shi, D., Xu, Y. and Morel, F. M. M.: Effects of the pH/pCO<sub>2</sub> control method on medium chemistry  
828 and phytoplankton growth, *Biogeosciences*, 6(7), 1199–1207, doi:10.5194/bg-6-1199-2009,  
829 2009.

830 Smetacek, V. and Cloern, J. E.: On Phytoplankton Trends, *Science* (80-. ), 319(5868), 1346–1348  
831 [online] Available from: <http://www.jstor.org/stable/20053523>, 2008.

832 Smyth, T. J., Fishwick, J. R., AL-Moosawi, L., Cummings, D. G., Harris, C., Kitidis, V., Rees, A.,  
833 Martinez-Vicente, V. and Woodward, E. M. S.: A broad spatio-temporal view of the Western  
834 English Channel observatory, *J. Plankton Res.*, 32(5), 585–601, doi:10.1093/plankt/fbp128,  
835 2010.

836 Strom, S.: Novel interactions between phytoplankton and microzooplankton : their influence on  
837 the coupling between growth and grazing rates in the sea, *Hydrobiologia* , 480, 41–54, 2002.

838 Tarran, G. A., Heywood, J. L. and Zubkov, M. V.: Latitudinal changes in the standing stocks of  
839 nano- and picoeukaryotic phytoplankton in the Atlantic Ocean, *Deep Sea Res. Part II Top. Stud.*  
840 *Oceanogr.*, 53(14–16), 1516–1529, doi:10.1016/j.dsr2.2006.05.004, 2006.

841 Taucher, J., Jones, J., James, A., Brzezinski, M. A., Carlson, C. A., Riebesell, U. and Passow, U.:  
842 Combined effects of CO<sub>2</sub> and temperature on carbon uptake and partitioning by the marine  
843 diatoms *Thalassiosira weissflogii* and *Dactyliosolen fragilissimus*, *Limnol. Oceanogr.*, 60(3), 901–  
844 919, doi:10.1002/lno.10063, 2015.

845 Thoisen, C., Riisgaard, K., Lundholm, N., Nielsen, T. and Hansen, P.: Effect of acidification on an  
846 Arctic phytoplankton community from Disko Bay, West Greenland, *Mar. Ecol. Prog. Ser.*, 520,  
847 21–34, doi:10.3354/meps11123, 2015.

848 Thomas, M. K., Kremer, C. T., Klausmeier, C. A. and Litchman, E.: A Global Pattern of Thermal  
849 Adaptation in Marine Phytoplankton, *Science* (80-. ), 338(6110), 1085–1088,  
850 doi:10.1126/science.1224836, 2012.

851 Torstensson, A., Chierici, M. and Wulff, A.: The influence of increased temperature and carbon  
852 dioxide levels on the benthic/sea ice diatom *Navicula directa*, *Polar Biol.*, 35(2), 205–214,  
853 doi:10.1007/s00300-011-1056-4, 2012.

854 Tortell, P., DiTullio, G., Sigman, D. and Morel, F.: CO<sub>2</sub> effects on taxonomic composition and  
855 nutrient utilization in an Equatorial Pacific phytoplankton assemblage, *Mar. Ecol. Prog. Ser.*, 236,  
856 37–43, doi:10.3354/meps236037, 2002.

857 Tortell, P. D., Payne, C. D., Li, Y., Trimborn, S., Rost, B., Smith, W. O., Riesselman, C., Dunbar, R. B.,  
858 Sedwick, P. and DiTullio, G. R.: CO<sub>2</sub> sensitivity of Southern Ocean phytoplankton, *Geophys. Res.*  
859 *Let.*, 35(4), L04605, doi:10.1029/2007GL032583, 2008.

860 Utermöhl, H.: Zur vervollkommnung der quantitativen phytoplankton-methodik, *Mitt. int. Ver.*  
861 *theor. angew. Limnol.*, 9, 1–38, 1958.

862 Verity, P. G., Brussaard, C. P., Nejtgaard, J. C., Van Leeuwe, M. a., Lancelot, C. and Medlin, L. K.:  
863 Current understanding of *Phaeocystis* ecology and biogeochemistry, and perspectives for future  
864 research, edited by M. A. van Leeuwe, J. Stefels, S. Belviso, C. Lancelot, P. G. Verity, and W. W. C.  
865 Gieskes, Springer Netherlands., 2007.

866 Webb, W. L., Newton, M. and Starr, D.: Carbon dioxide exchange of *Alnus rubra*, *Oecologia*, 17(4),  
867 281–291, doi:10.1007/BF00345747, 1974.

868 Welschmeyer: Fluorometric analysis of chlorophyll a in the presence of chlorophyll b and  
869 pheopigments, *Limnol. Oceanogr.*, 39(8), 1985–1992, 1994.

870 Widdicombe, C. E., Eloire, D., Harbour, D., Harris, R. P. and Somerfield, P. J.: Long-term  
871 phytoplankton community dynamics in the Western English Channel, *J. Plankton Res.*, 32(5),  
872 643–655, doi:10.1093/plankt/fbp127, 2010a.

873 Wolf-gladrow, B. D. A., Riebesell, U. L. F., Burkhardt, S. and Jelle, B.: Direct effects of CO<sub>2</sub>  
874 concentration on growth and isotopic composition of marine plankton, *Tellus*, 51B, 461–476,  
875 1999.

876 Woods, H. A. and Harrison, J. F.: Temperature and the chemical composition of poikilothermic  
877 organisms, , (Sidell 1998), 237–245, 2003.

878

879

880

881

882

883

884

885

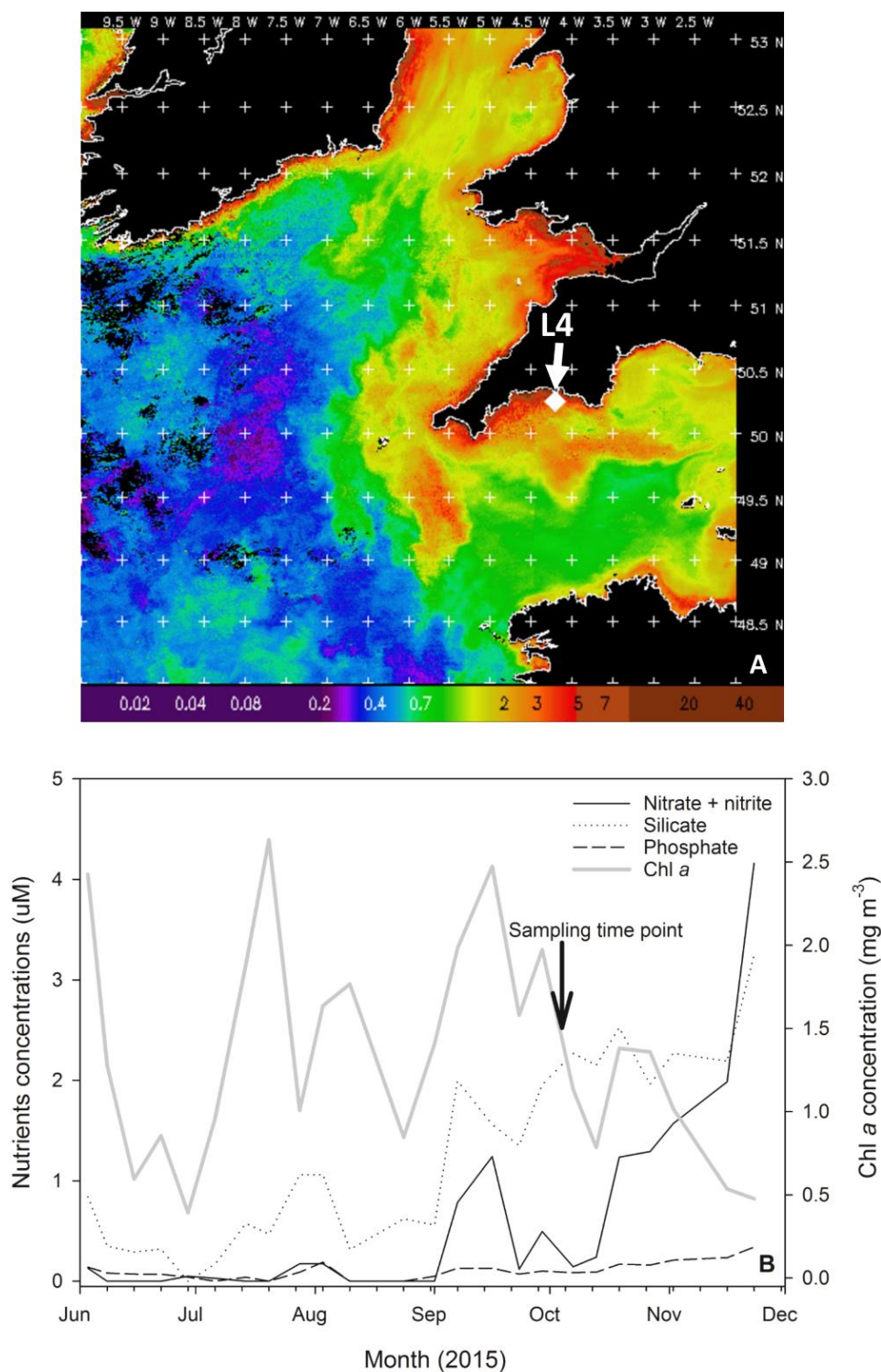


**Fig. 1.** (A). MODIS weekly composite chl *a* image of the western English Channel covering the period 30<sup>th</sup> September – 6<sup>th</sup> October 2015 (coincident with the week of phytoplankton community sampling for the present study), processing courtesy of NEODAAS. The position of coastal station L4 is marked with a white diamond. (B). Profiles of weekly nutrient and chl *a* concentrations from station L4 at a depth of 10 m over the second half of 2015 in the months prior to phytoplankton community sampling (indicated by black arrow and text).

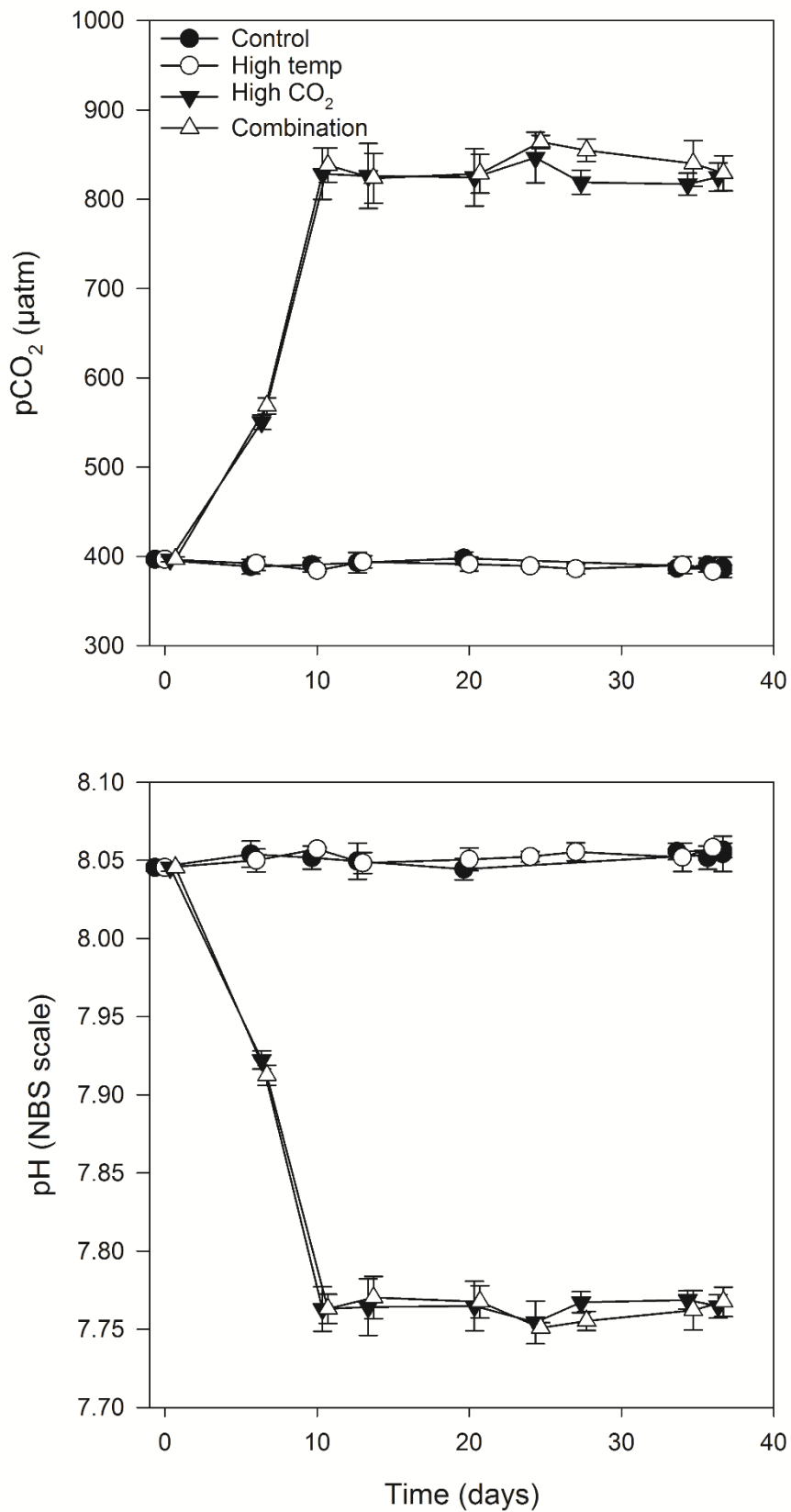


**Fig. 2.** Calculated values of partial pressure of CO<sub>2</sub> in seawater (pCO<sub>2</sub>) (A) and pH (B) from direct measurements of total alkalinity and dissolved inorganic carbon. (For full carbonate system values see **Table S1.**, supplementary material)

888

889

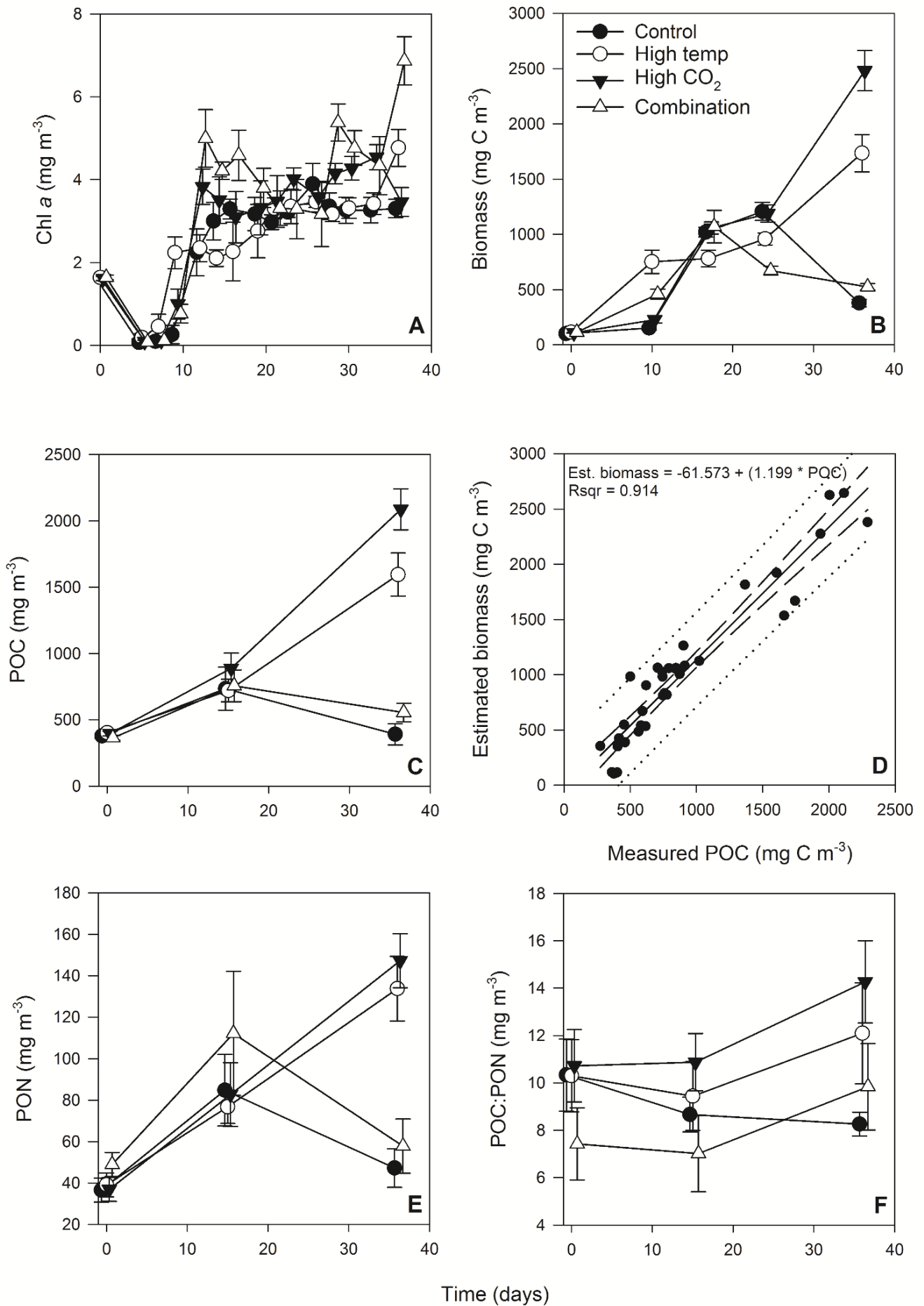


**Fig. 3.** Time course of chl *a* (A), estimated phytoplankton biomass (B), POC (C), regression of estimated phytoplankton carbon vs measured POC (D), PON (E) and POC:PON (F).

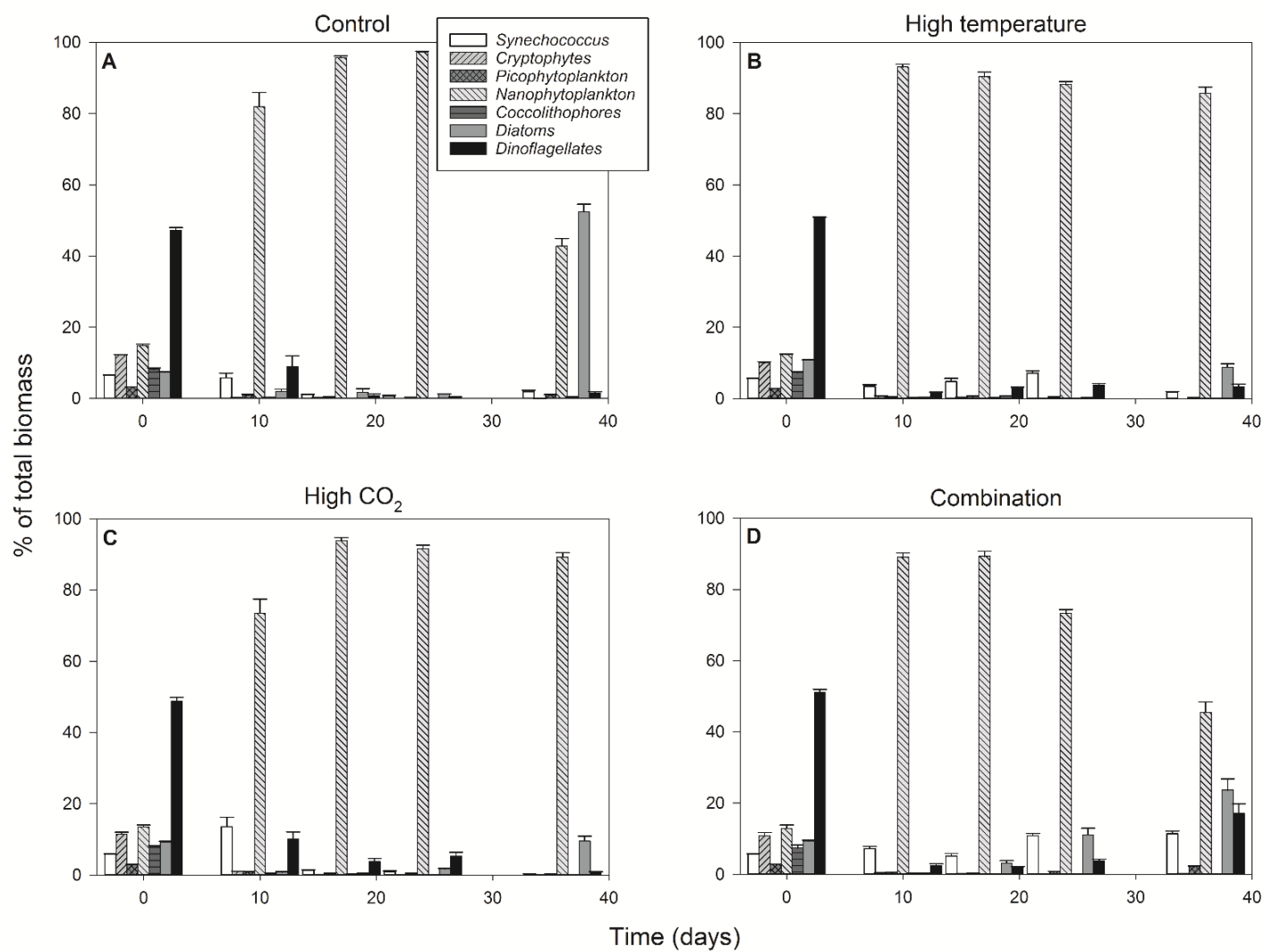


**Fig. 4.** Percentage contribution to community biomass by phytoplankton groups/species throughout the experiment in the control (A), high temperature (B), high CO<sub>2</sub> (C) and combination treatments (D).

891

892

893

894

895

896

897

898

899

900

901

902

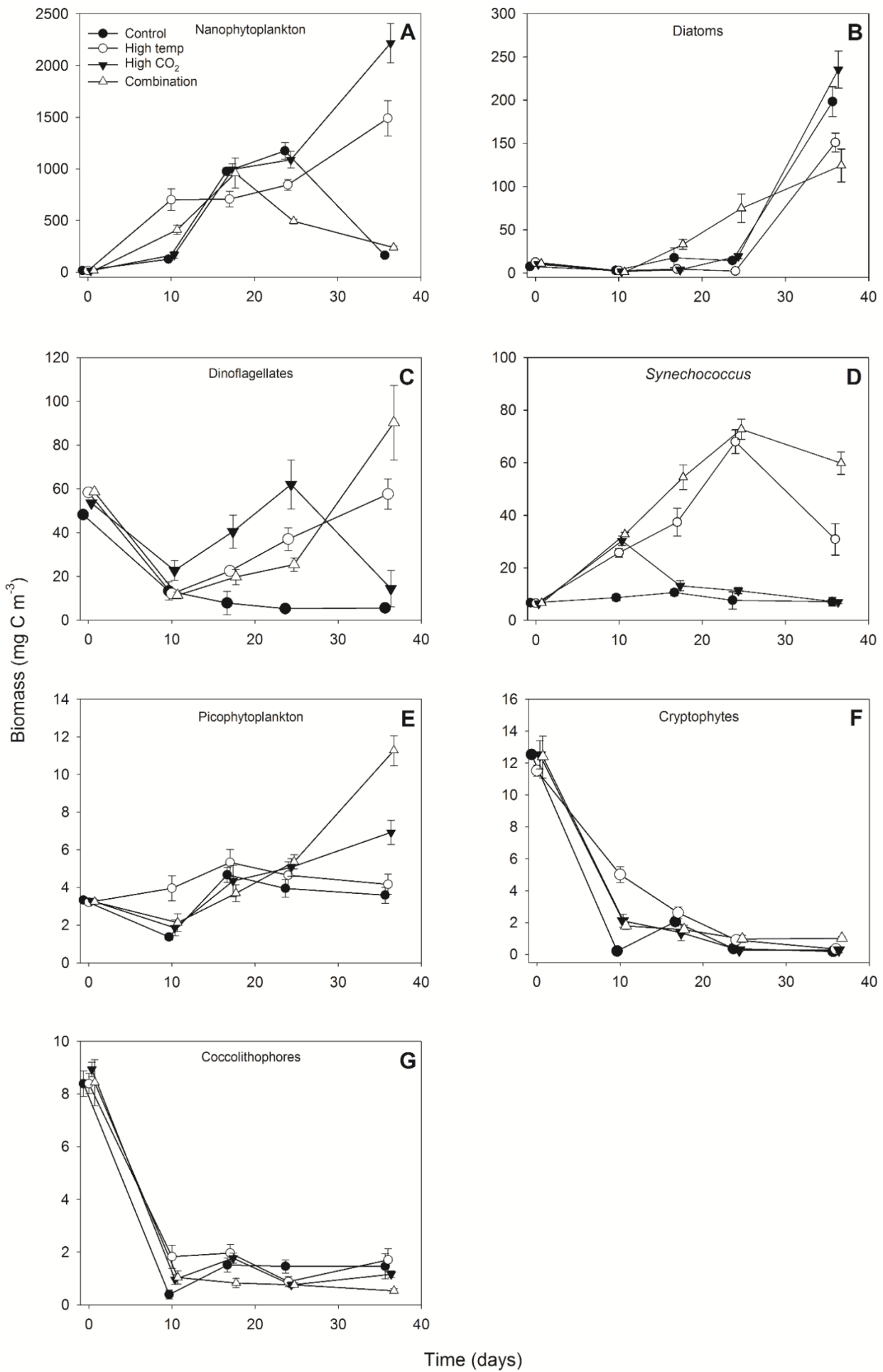


**Fig. 5.** Response of individual phytoplankton groups to experimental treatments.



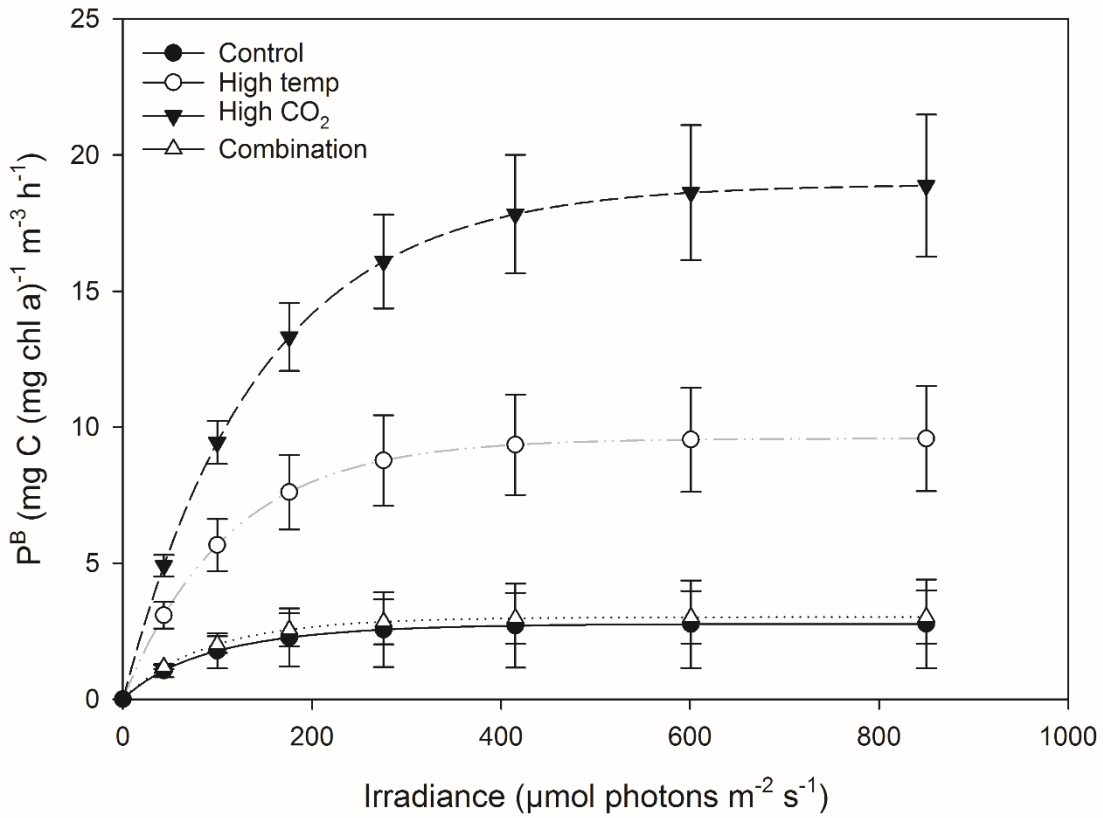


**Fig. 6.** Fitted parameters of FRRf-based photosynthesis-irradiance curves for the experimental treatments on the final experimental day (T36)

903  
 904  
 905  
 906  
 907  
 908  
 909  
 910  
 911  
 912  
 913  
 914  
 915

916  
917  
918

**Table 1.** Results of generalized linear mixed model testing for effects of time, temperature, pCO<sub>2</sub> and all interactions on chl *a*, phytoplankton biomass and particulate organic carbon and nitrogen. Significant results are in bold; \* p < 0.05, \*\* p < 0.01, \*\*\* p < 0.001.

| <u>Response variable</u>                              | <u>n</u> | <u>df</u> | <u>z-value</u> | <u>p</u>         | <u>sig</u> |
|---|----------|-----------|----------------|------------------|------------|
| <b><u>Chla (mg m<sup>-3</sup>)</u></b>                |          |           |                |                  |            |
| High temp   | 516      | 507       | 0.412          | 0.680            |            |
| High pCO <sub>2</sub>                                 | 516      | 507       | 0.664          | 0.507            |            |
| Time  | 516      | 507       | 3.815          | <b>&lt;0.001</b> | ***        |
| High temp x high pCO <sub>2</sub>                     | 516      | 507       | 1.100          | 0.271            |            |
| Time x high temp                                      | 516      | 507       | -0.213         | 0.831            |            |
| Time x high CO <sub>2</sub>                           | 516      | 507       | -0.011         | 0.991            |            |
| Time x high temp x high CO <sub>2</sub>               | 516      | 507       | 0.340          | 0.734            |            |
| <b><u>Estimated biomass (mg C m<sup>-3</sup>)</u></b> |          |           |                |                  |            |
| High temp   | 80       | 71        | 0.092          | 0.927            |            |
| High pCO <sub>2</sub>                                 | 80       | 71        | 2.102          | <b>0.036</b>     | *          |
| Time  | 80       | 71        | 2.524          | <b>0.012</b>     | *          |
| High temp x high pCO <sub>2</sub>                     | 80       | 71        | 1.253          | 0.210            |            |
| Time x high temp                                      | 80       | 71        | 1.866          | 0.062            |            |
| Time x high CO <sub>2</sub>                           | 80       | 71        | 4.414          | <b>&lt;0.001</b> | ***        |
| Time x high temp x high CO <sub>2</sub>               | 80       | 71        | -1.050         | 0.294            |            |
| <b><u>POC (mg m<sup>-3</sup>)</u></b>                 |          |           |                |                  |            |
| High temp   | 48       | 38        | -0.977         | 0.328            |            |
| High pCO <sub>2</sub>                                 | 48       | 38        | -0.866         | 0.386            |            |
| Time  | 48       | 38        | -0.203         | 0.839            |            |
| High temp x high pCO <sub>2</sub>                     | 48       | 38        | -0.29          | 0.772            |            |
| Time x high temp                                      | 48       | 38        | 3.648          | <b>&lt;0.001</b> | ***        |
| Time x high CO <sub>2</sub>                           | 48       | 38        | 4.333          | <b>&lt;0.001</b> | ***        |
| Time x high temp x high CO <sub>2</sub>               | 48       | 38        | 0.913          | 0.361            |            |
| <b><u>PON (mg m<sup>-3</sup>)</u></b>                 |          |           |                |                  |            |
| High temp   | 48       | 38        | -0.640         | 0.522            |            |
| High pCO <sub>2</sub>                                 | 48       | 38        | -0.479         | 0.632            |            |
| Time  | 48       | 38        | 0.202          | 0.84             |            |
| High temp x high pCO <sub>2</sub>                     | 48       | 38        | 0.667          | 0.505            |            |
| Time x high temp                                      | 48       | 38        | 1.674          | 0.094            |            |
| Time x high CO <sub>2</sub>                           | 48       | 38        | 2.037          | <b>&lt; 0.05</b> | *          |
| Time x high temp x high CO <sub>2</sub>               | 48       | 38        | -0.141         | 0.730            |            |
| <b><u>POC:PON (mg m<sup>-3</sup>)</u></b>             |          |           |                |                  |            |
| High temp   | 48       | 38        | 0.222          | 0.824            |            |
| High pCO <sub>2</sub>                                 | 48       | 38        | 0.029          | 0.977            |            |
| Time  | 48       | 38        | 0.249          | 0.803            |            |
| High temp x high pCO <sub>2</sub>                     | 48       | 38        | 0.990          | 0.322            |            |
| Time x high temp                                      | 48       | 38        | 2.377          | <b>0.017</b>     | *          |
| Time x high CO <sub>2</sub>                           | 48       | 38        | 2.748          | <b>0.006</b>     | **         |
| Time x high temp x high CO <sub>2</sub>               | 48       | 38        | -0.215         | 0.830            |            |

919

920  
921  
922

**Table 2.** Results of generalized linear mixed model testing for significant effects of time, temperature, pCO<sub>2</sub> and all interactions on phytoplankton species biomass. Significant results are in bold;

\* p < 0.05, \*\* p < 0.01, \*\*\* p < 0.001.

| <b>Response variable</b>                      | <b>n</b> | <b>df</b> | <b>z-value</b> | <b>p</b>         | <b>sig</b> |
|---|----------|-----------|----------------|------------------|------------|
| <b>Diatoms (mg C m<sup>-3</sup>)</b>          |          |           |                |                  |            |
| High temp                                     | 80       | 70        | -0.216         | 0.829            |            |
| High pCO <sub>2</sub>                         | 80       | 70        | -0.895         | 0.371            |            |
| Time  | 80       | 70        | 2.951          | <b>0.003</b>     | <b>**</b>  |
| High temp x high pCO <sub>2</sub>             | 80       | 70        | 1.063          | 0.288            |            |
| Time x high temp                              | 80       | 70        | -1.151         | 0.250            |            |
| Time x high CO <sub>2</sub>                   | 80       | 70        | 0.560          | 0.576            |            |
| Time x high temp x high CO <sub>2</sub>       | 80       | 70        | 0.368          | 0.713            |            |
| <b>Dinoflagellates (mg C m<sup>-3</sup>)</b>  |          |           |                |                  |            |
| High temp                                     | 80       | 70        | -0.018         | 0.986            |            |
| High pCO <sub>2</sub>                         | 80       | 70        | 0.487          | 0.627            |            |
| Time  | 80       | 70        | -2.347         | <b>0.019</b>     | <b>*</b>   |
| High temp x high pCO <sub>2</sub>             | 80       | 70        | -0.166         | 0.868            |            |
| Time x high temp                              | 80       | 70        | 1.857          | 0.063            |            |
| Time x high CO <sub>2</sub>                   | 80       | 70        | 1.009          | 0.313            |            |
| Time x high temp x high CO <sub>2</sub>       | 80       | 70        | 2.207          | <b>0.027</b>     | <b>*</b>   |
| <b>Nanophytoplankton (mg m<sup>-3</sup>)</b>  |          |           |                |                  |            |
| High temp                                     | 80       | 70        | -0.371         | 0.710            |            |
| High pCO <sub>2</sub>                         | 80       | 70        | -2.108         | <b>0.035</b>     | <b>*</b>   |
| Time  | 80       | 70        | 2.162          | <b>0.031</b>     | <b>*</b>   |
| High temp x high pCO <sub>2</sub>             | 80       | 70        | 0.79           | 0.430            |            |
| Time x high temp                              | 80       | 70        | 1.695          | 0.090            |            |
| Time x high CO <sub>2</sub>                   | 80       | 70        | 3.563          | <b>&lt;0.001</b> | <b>***</b> |
| Time x high temp x high CO <sub>2</sub>       | 80       | 70        | -0.806         | 0.420            |            |
| <b>Synechococcus (mg m<sup>-3</sup>)</b>      |          |           |                |                  |            |
| High temp                                     | 80       | 70        | 3.333          | <b>&lt;0.001</b> | <b>***</b> |
| High pCO <sub>2</sub>                         | 80       | 70        | 2.231          | <b>0.026</b>     | <b>*</b>   |
| Time  | 80       | 70        | 0.049          | 0.961            |            |
| High temp x high pCO <sub>2</sub>             | 80       | 70        | 2.391          | <b>0.017</b>     | <b>*</b>   |
| Time x high temp                              | 80       | 70        | 4.076          | <b>&lt;0.001</b> | <b>***</b> |
| Time x high CO <sub>2</sub>                   | 80       | 70        | -1.553         | 0.1204           |            |
| Time x high temp x high CO <sub>2</sub>       | 80       | 70        | 5.382          | <b>&lt;0.001</b> | <b>***</b> |
| <b>Picophytoplankton (mg m<sup>-3</sup>)</b>  |          |           |                |                  |            |
| High temp                                     | 80       | 70        | 0.951          | 0.342            |            |
| High pCO <sub>2</sub>                         | 80       | 70        | -0.472         | 0.637            |            |
| Time  | 80       | 70        | 0.897          | 0.370            |            |
| High temp x high pCO <sub>2</sub>             | 80       | 70        | -1.188         | 0.235            |            |
| Time x high temp                              | 80       | 70        | -0.219         | 0.827            |            |
| Time x high CO <sub>2</sub>                   | 80       | 70        | 1.411          | 0.158            |            |
| Time x high temp x high CO <sub>2</sub>       | 80       | 70        | 2.792          | <b>0.005</b>     | <b>**</b>  |
| <b>Coccolithophores (mg C m<sup>-3</sup>)</b> |          |           |                |                  |            |
| High temp                                     | 80       | 70        | -0.408         | 0.683            |            |
| High pCO <sub>2</sub>                         | 80       | 70        | -0.308         | 0.758            |            |
| Time  | 80       | 70        | 0.211          | 0.833            |            |

**Table 2 cont'd.**

|   |    |    |        |                  |            |
|---|----|----|--------|------------------|------------|
| High temp x high pCO <sub>2</sub>         | 80 | 70 | -0.319 | 0.750            |            |
| Time x high temp                          | 80 | 70 | 0.269  | 0.788            |            |
| Time x high CO <sub>2</sub>               | 80 | 70 | 0.295  | 0.768            |            |
| Time x high temp x high CO <sub>2</sub>   | 80 | 70 | 0.502  | 0.615            |            |
| <b>Cryptophytes (mg C m<sup>-3</sup>)</b> |    |    |        |                  |            |
| High temp                                 | 80 | 70 | 0.207  | 0.836            |            |
| High pCO <sub>2</sub>                     | 80 | 70 | 0.256  | 0.798            |            |
| Time                                      | 80 | 70 | -5.289 | <b>&lt;0.001</b> | <b>***</b> |
| High temp x high pCO <sub>2</sub>         | 80 | 70 | -0.349 | 0.727            |            |
| Time x high temp                          | 80 | 70 | 1.885  | 0.059            |            |
| Time x high CO <sub>2</sub>               | 80 | 70 | 0.167  | 0.867            |            |
| Time x high temp x high CO <sub>2</sub>   | 80 | 70 | 1.694  | 0.090            |            |

923

924

925

926

927

928

929

930

931

**Table 3.** FRRf-based photosynthesis-irradiance curve parameters for the experimental treatments on the final day (T36).

| Parameter                        | Control | sd    | High temp | sd   | High CO <sub>2</sub> | sd    | Combination | sd    |
|----------------------------------|---------|-------|-----------|------|----------------------|-------|-------------|-------|
| <b>P<sup>B</sup><sub>m</sub></b> | 2.77    | 1.63  | 9.58      | 1.94 | 18.93                | 2.65  | 3.02        | 0.97  |
| <b>α</b>                         | 0.03    | 0.01  | 0.09      | 0.01 | 0.13                 | 0.01  | 0.04        | 0.00  |
| <b>I<sub>k</sub></b>             | 85.33   | 45.47 | 110.93    | 6.09 | 144.13               | 17.91 | 86.38       | 33.06 |

932

933

934

935

936

937

938

939

940

941

942 **Table 4.** Results of generalised linear model testing for significant effects of temperature, CO<sub>2</sub> and temperature  
 943 x CO<sub>2</sub> on phytoplankton photophysiology at T36; P<sup>B</sup><sub>m</sub> (maximum photosynthetic rates), α (light limited slope)  
 944 and I<sub>k</sub> (light saturated photosynthesis). Significant results are in bold; \* p < 0.05, \*\* p < 0.001, \*\*\* p < 0.0001.

| <b>Response variable</b>                | <b>n</b> | <b>df</b> | <b>t-value</b> | <b>p</b>        | <b>sig</b> |
|---|----------|-----------|----------------|-----------------|------------|
| <b><u>P<sup>B</sup><sub>m</sub></u></b> |          |           |                |                 |            |
| High temp                               | 12       | 8         | 7.353          | < <b>0.0001</b> | ***        |
| High pCO <sub>2</sub>                   | 12       | 8         | 8.735          | < <b>0.0001</b> | ***        |
| High temp x high pCO <sub>2</sub>       | 12       | 8         | -8.519         | < <b>0.0001</b> | ***        |
| <b><u>α</u></b>                         |          |           |                |                 |            |
| High temp                               | 12       | 8         | 13.03          | < <b>0.0001</b> | ***        |
| High pCO <sub>2</sub>                   | 12       | 8         | 15.15          | < <b>0.0001</b> | ***        |
| High temp x high pCO <sub>2</sub>       | 12       | 8         | -14.82         | < <b>0.0001</b> | ***        |
| <b><u>I<sub>k</sub></u></b>             |          |           |                |                 |            |
| High temp                               | 12       | 8         | 2.018          | 0.0783          |            |
| High pCO <sub>2</sub>                   | 12       | 8         | 2.541          | <b>0.0347</b>   | *          |
| High temp x high pCO <sub>2</sub>       | 12       | 8         | -2.441         | <b>0.0405</b>   | *          |

945

946

947